



Role of Dicer-Dependent RNA Interference in Regulating Mycoparasitic Interactions

Edoardo Piombo,^a  Ramesh R. Vetukuri,^b Anders Broberg,^c Pruthvi B. Kalyandurg,^b Sandeep Kushwaha,^{b,d} Dan Funck Jensen,^a Magnus Karlsson,^a  Mukesh Dubey^a

^aDepartment of Forest Mycology and Plant Pathology, Swedish University of Agricultural Sciences, Uppsala, Sweden

^bDepartment of Plant Breeding, Horticum, Swedish University of Agricultural Sciences, Lomma, Sweden

^cDepartment of Molecular Sciences, Swedish University of Agricultural Sciences, Uppsala, Sweden

^dNational Institute of Animal Biotechnology, Hyderabad, Telangana, India

ABSTRACT Dicer-like proteins (DCLs) play a vital role in RNA interference (RNAi), by cleaving RNA filament into small RNAs. Although DCL-mediated RNAi can regulate interspecific communication between pathogenic/mutualistic organisms and their hosts, its role in mycoparasitic interactions is yet to be investigated. In this study, we deleted *dcl* genes in the mycoparasitic fungus *Clonostachys rosea* and characterize the functions of DCL-dependent RNAi in mycoparasitism. Deletion of *dcl2* resulted in a mutant with reduced secondary metabolite production, antagonism toward the plant-pathogenic fungus *Botrytis cinerea*, and reduced ability to control *Fusarium* foot rot disease on wheat, caused by *Fusarium graminearum*. Transcriptome sequencing of the *in vitro* interaction between the *C. rosea* $\Delta dcl2$ strain and *B. cinerea* or *F. graminearum* identified the downregulation of genes coding for transcription factors, membrane transporters, hydrolytic enzymes, and secondary metabolites biosynthesis enzymes putatively involved in antagonistic interactions, in comparison with the *C. rosea* wild-type interaction. A total of 61 putative novel microRNA-like RNAs (miRNAs) were identified in *C. rosea*, and 11 were downregulated in the $\Delta dcl2$ mutant. In addition to putative endogenous gene targets, these miRNAs were predicted to target *B. cinerea* and *F. graminearum* virulence factor genes, which showed an increased expression during interaction with the $\Delta dcl2$ mutant incapable of producing the targeting miRNAs. In summary, this study constitutes the first step in elucidating the role of RNAi in mycoparasitic interactions, with important implications for biological control of plant diseases, and poses the base for future studies focusing on the role of cross-species RNAi regulating mycoparasitic interactions.

IMPORTANCE Small RNAs mediated RNA interference (RNAi) known to regulate several biological processes. Dicer-like endoribonucleases (DCLs) play a vital role in the RNAi pathway by generating sRNAs. In this study, we investigated a role of DCL-mediated RNAi in interference interactions between mycoparasitic fungus *Clonostachys rosea* and the two fungal pathogens *Botrytis cinerea* and *Fusarium graminearum* (here called mycohosts). We found that the *dcl* mutants were not able to produce 11 sRNAs predicted to finetune the regulatory network of genes known to be involved in production of hydrolytic enzymes, antifungal compounds, and membrane transporters needed for antagonistic action of *C. rosea*. We also found *C. rosea* sRNAs putatively targeting known virulence factors in the mycohosts, indicating RNAi-mediated cross-species communication. Our study expanded the understanding of underlying mechanisms of cross-species communication during interference interactions and poses a base for future works studying the role of DCL-based cross-species RNAi in fungal interactions.

KEYWORDS antagonism, biocontrol, *Clonostachys rosea*, gene regulation, mycoparasitism, RNA interference, small RNA

Citation Piombo E, Vetukuri RR, Broberg A, Kalyandurg PB, Kushwaha S, Funck Jensen D, Karlsson M, Dubey M. 2021. Role of Dicer-dependent RNA interference in regulating mycoparasitic interactions. *Microbiol Spectr* 9: e01099-21. <https://doi.org/10.1128/Spectrum.01099-21>.

Editor Christina A. Cuomo, Broad Institute

Copyright © 2021 Piombo et al. This is an open-access article distributed under the terms of the [Creative Commons Attribution 4.0 International license](https://creativecommons.org/licenses/by/4.0/).

Address correspondence to Mukesh Dubey, Mukesh.dubey@slu.se.

 small RNAs in mycoparasitic interactions

Received 29 July 2021

Accepted 11 August 2021

Published 22 September 2021

Small RNAs (sRNAs) are a group of noncoding RNAs. They play a central role in gene silencing at the transcriptional level through chromatin modification and at the post-transcriptional level through targeted destruction of mRNAs, also known as RNA interference (RNAi) (1–5). Dicer-like protein (DCL) plays central role in RNAi by cleaving the double-stranded RNA precursors and single-stranded RNA precursors with hairpin structures to generate sRNAs, often ranging in size from 18 to 40 nucleotides, called small-interfering RNAs (siRNAs) and microRNAs (miRNAs; microRNA-like RNAs [miRNAs] in fungi), respectively. In fungi, the most studied RNAi pathways are mediated by siRNAs and miRNAs and are dependent on DCLs for biogenesis and are thus called Dicer-dependent RNAi. Dicer-independent RNAi, such as that mediated by dicer-independent small interfering RNAs (disiRNAs), has also been identified in the filamentous fungus *Neurospora crassa* (6).

Small-RNA mediated RNAi is an evolutionarily conserved process of self-defense triggered by a wide variety of exogenous nucleic acids such as invading viruses, transgenes, transposons, and plasmids (7, 8). In fungi, a role of sRNA-mediated RNAi pathways in genome defense against the insertion of repetitive transgenes during vegetative growth (quelling) and the sexual phase of the life cycle (meiotic silencing of unpaired DNA [MSUD]) was first reported in *N. crassa* (9–11). Since then, RNAi pathways and their role in genome defense against retrotransposon activity have been demonstrated in several fungal species with diverse lifestyles (8, 12–20). However, in some fungal species, such as *Saccharomyces cerevisiae* and *Ustilago maydis*, genes related to the RNAi pathways are absent (21, 22). In addition to the role of genome defense against transgenes, the fungal RNAi machinery generates a variety of sRNAs that are involved in the regulation of numerous biological processes through targeted gene silencing (8, 23). For instance, sRNAs (mainly miRNAs) are found to be differentially expressed in fungi during different growth phases, developmental stages, and environmental conditions, including those involved in host-pathogen interactions (24–34). Furthermore, sRNAs can move bidirectionally between the species and modulate cellular functions of recipient cells by hijacking their RNAi machinery. Thus, they play an important role in interspecies communication between closely interacting symbiotic organisms, including parasitic and mutualistic interactions (35–40). However, the role of sRNAs in parasitic fungus-fungus interactions is yet to be investigated.

The filamentous fungus *Clonostachys rosea* is a ubiquitous soilborne ascomycete with a complex lifestyle as a necrotrophic mycoparasite and saprotroph (41). *C. rosea* efficiently overgrows and kills its mycohosts such as *Botrytis cinerea* and *Fusarium graminearum* (41–43). During mycoparasitic interactions or exposure to the secreted factors from mycohosts, *C. rosea* induces expression of genes associated with the production of secondary metabolites, hydrolytic enzymes, and other secreted proteins (43–50). Furthermore, *C. rosea* induces expression of genes coding for membrane transporters to efflux the endogenous toxic compounds and exogenous metabolites that may come from interacting organisms during the interspecific interactions (49, 51, 52). The role of secreted proteins/enzymes, secondary metabolites, and membrane transporters in antibiosis and mycoparasitism in *C. rosea* is proven (42–44, 50, 53, 54); however, the role of RNAi in regulating the cellular regulatory network during such interactions has not yet been investigated.

The present work aims to (i) characterize the RNAi machinery in *C. rosea*; (ii) identify miRNAs that are key regulators of genes associated with the antagonistic/mycoparasitic activity in *C. rosea*, as well as their potential endogenous and cross-species gene targets; and (iii) investigate common or species-specific responses in sRNA-mediated gene regulation in *C. rosea* against mycohosts. We used the two important plant-pathogenic fungi *B. cinerea* and *F. graminearum* as different mycohosts, since they are taxonomically different from each other and represent different disease types on different crops. We hypothesized that (i) sRNAs regulate mycoparasitic interactions in *C. rosea* at endogenous and cross-species level and that (ii) *C. rosea* responds with both common and mycohost-specific reactions toward *B. cinerea* and *F. graminearum*. To test these hypotheses, we generated gene deletion and complementation strains of genes

coding for DCL proteins (DCL1 and DCL2) in *C. rosea* and used a holistic approach (sRNA, transcriptome, and secondary metabolome analysis) to investigate the sRNA-mediated regulatory network and its influence on mycoparasitic fungus-fungus interactions at endogenous and cross-species level.

RESULTS

Identification and sequence analysis of the predicted RNAi machinery in *C. rosea*.

Genes coding for different protein components involved in the RNAi pathway were identified through BLAST analysis of *C. rosea* strain IK726 genome version 1 (41) and version 2 (55) using *N. crassa* and *Trichoderma atroviride* argonout (AGO), DCL, and RNA dependent RNA polymerase (RDR) gene sequences as queries. Two AGO (AGO1, protein ID CRV2G00002735; AGO2, protein ID CRV2G00000975), two DCL (DCL1, protein ID CRV2G00009872; DCL2 protein ID CRV2G00008135), and three RDR (RDR1, protein ID CRV2G00001186; RDR2, protein ID CRV2G00002170; RDR3, protein ID CRV2G00007201) genes were identified in the *C. rosea* genome. Analysis of the translated amino acid sequences for the presence of conserved modules identified the domains known to be present in DCL (DEXDc, HELICc, Dicer dimer, and RNase III), AGO (ArgoN, DUF, PAZ, ArgoL2, and PIWI), and RDR proteins (see Fig. S2B in the supplemental material). The characteristics of *C. rosea* AGOs, DCLs, and RDRs are presented in Table S1C.

Phylogenetic analyses using DCL, AGO, and RDR amino acid sequences revealed that *C. rosea* putative DCLs were most closely related to their homologs in *Acremonium chrysogenum*, with around 57% sequence identity, and the same was true for *C. rosea* homologs of AGO1 and AGO2, but with an identity around 51%. The three putative RDR genes were similar to their homologs in *A. chrysogenum* as well, with identities of 37, 42, and 55%, respectively. In the phylogenetic analyses, the putative DCLs of *C. rosea* diverged in two clusters separating the DCL1 and DCL2 from the analyzed species (see Fig. S2C), and the same was evident for AGO1 and AGO2 (see Fig. S2D). The tree generated from the RDR sequences formed by three main clusters, each containing one of the *C. rosea* proteins (see Fig. S2E). Our data therefore suggest that *C. rosea* contain two DCL, two AGO, and three RDR genes, with clear orthologs in related species.

Generation of gene deletion and complementation strains. To investigate the biological roles of RNAi in *C. rosea*, genes encoding DCL proteins were selected for gene deletions as they act upstream in the RNAi pathways. Single *dcl1* and *dcl2* deletion strains ($\Delta dcl1$ and $\Delta dcl2$) were generated, and they were successfully complemented with *dcl1* and *dcl2*, respectively, to generate $\Delta dcl1+$ and $\Delta dcl2+$ complementation strains. Results describing validation of gene deletion and complementation strains are presented in Fig. S1. Phenotypic analyses experiments were performed with *C. rosea* wild-type (WT), *dcl* deletion strains ($\Delta dcl1$ and $\Delta dcl2$) and their respective $\Delta dcl1+$ and $\Delta dcl2+$ complemented strains.

Deletion of *dcl* affects growth, conidiation, antagonism, and biocontrol. The growth rate of the $\Delta dcl2$ strain was 14% lower ($P < 0.001$) than the WT growth rate on potato dextrose agar (PDA), while no significant difference was found between the $\Delta dcl1$ strain and the WT (Fig. 1A). No significant difference in mycelial biomass ($P \leq 0.36$) between the *C. rosea* WT and the *dcl* deletion strains was found (see Fig. S3A). We quantified the conidiation of *C. rosea* WT and deletion strains 24 days postinoculation (dpi). At this time, the colony perimeter of each strain had reached the edge of the 9-cm petri dish. Conidium production for the $\Delta dcl1$ strain was 70% higher ($P = 0.014$) than that of the WT, while no significant ($P = 0.75$) difference in conidia yield was recorded in the $\Delta dcl2$ strain (Fig. 1B). Complementation $\Delta dcl1+$ strains showed partial restoration of the conidial production phenotype observed in $\Delta dcl1$. Morphological examination during growth on PDA revealed that the $\Delta dcl2$ strain had reduced ability to produce yellow pigment, while this phenotype remained unaffected in the $\Delta dcl1$ strain (Fig. 1C). No other marked difference in colony morphology was observed between the WT and the *dcl* deletion strains.

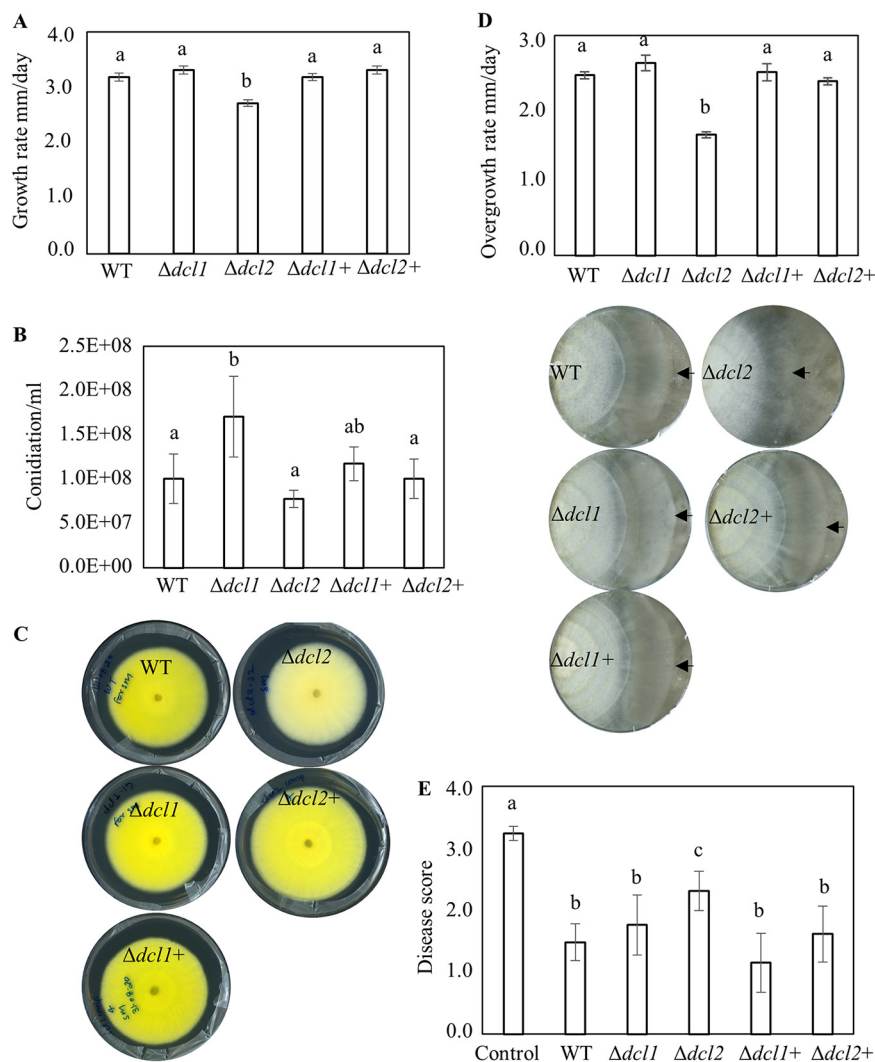


FIG 1 Phenotypic characterizations of *C. rosea* WT, deletion, and complementation strains. (A) Growth rate of WT, *dcl* deletion, and complemented strains. Strains were inoculated on PDA medium and incubated at 25°C, and the growth rate was recorded 5 days postinoculation (dpi). Error bars represent standard deviations based on four biological replicates. (B) Conidiation of WT, *dcl* deletion, and complementation strains on PDA medium 24 dpi. Conidia were harvested in equal volumes of water and were counted using a Bright-Line Haemocytometer according to the instructions of manufacturer. Error bars represent standard deviations based on four biological replicates. (C) Deletion of *dcl2* affects pigment production in *C. rosea*. Strains were inoculated on PDA medium and incubated at 25°C. The experiment was performed in four biological replicates, and photographs of representative plates were taken 16 dpi. (D) Dual culture assay to test antagonistic ability of *C. rosea* WT, deletion, and complementation strains against *B. cinerea*. Agar plugs of *C. rosea* strains (left side in the plate) and *B. cinerea* (right side in the plate) were inoculated on opposite sides in 9-cm-diameter agar plates, followed by incubation at 25°C. The growth rates (overgrowth) of *C. rosea* WT, deletion, and complementation strains on *B. cinerea* were measured from the point of mycelial contact. The experiment was performed in four replicates, and photographs of representative plates were taken 21 dpi of *C. rosea* strains. An arrowhead indicates the mycelial front of *C. rosea* strains. (E) *In vivo* assay to test the biocontrol ability of *C. rosea* strains against *F. graminearum* foot rot disease on wheat. Seeds were coated with *C. rosea* conidia and planted in moist sand together with a *F. graminearum* agar plug. Seedlings were harvested 21 dpi, and disease symptoms were scored on a scale from 0 to 4. The experiment was performed in five biological replicates with 15 plants in each replicate. Different letters indicate statistically significant differences based on Tukey HSD method at the 95% significance level.

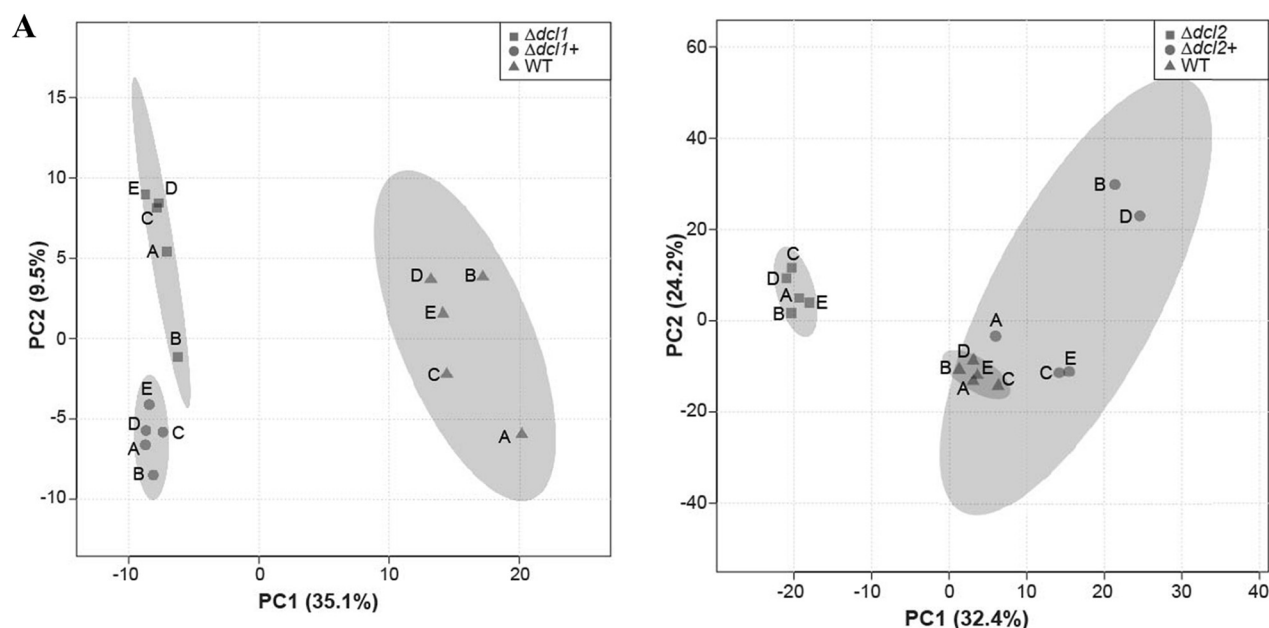
An *in vitro* dual culture assay was used to test whether deletion of *dcl1* or *dcl2* affected the antagonistic ability of *C. rosea*. No differences in growth rate of *F. graminearum* or *B. cinerea* were recorded during *in vitro* dual plate confrontation with either of the *dcl* deletion strains, compared to the WT (see Fig. S3A). However, a reduced ability

($P < 0.001$) to overgrow *B. cinerea* was observed in $\Delta dcl2$ strains compared to the WT (Fig. 1D). The growth rate of $\Delta dcl2$ strains displayed 33% reduction on *B. cinerea* mycelium (overgrowth rate) compared to the growth rate of WT (Fig. 1D). In contrast, overgrowth of *F. graminearum* was not compromised in either of the deletion strains (see Fig. S3A). However, a change in *F. graminearum* color (pigment) was visible at the bottom side of the $\Delta dcl2$ mutant-*F. graminearum* interaction zone (see Fig. S3A). In contrast to *in vitro* antagonism tests, a bioassay for biocontrol of *fusarium* foot rot diseases on wheat caused by *F. graminearum* displayed a significant 56% increase ($P = 0.023$) of disease severity in wheat seedlings previously seed coated with the $\Delta dcl2$ strain compared to seedlings from seeds coated with *C. rosea* WT (Fig. 1E). However, disease symptoms on seedlings from seeds coated with $\Delta dcl1$ strains showed no significant difference compared to the WT.

Analysis of metabolites. The metabolites produced by the WT, *dcl* deletion, and complementation strains were analyzed by ultrahigh-performance liquid chromatography/mass spectrometry (UHPLC-MS) and UHPLC-tandem MS (UHPLC-MS/MS) (see Table S2). When analyzing the UHPLC-MS data by principal-component analysis (PCA), the samples from the $\Delta dcl1$, $\Delta dcl1+$, and WT strains grouped separated from each other (Fig. 2A, left) and, likewise, $\Delta dcl2$ and WT samples clustered separately (Fig. 2A, right). The $\Delta dcl2+$ samples, however, clustered with the WT samples, indicating restoration of metabolite production in $\Delta dcl2+$ strains. Two compounds were present in significantly smaller amounts in the $\Delta dcl1$ strain, and their production was restored in $\Delta dcl1+$ strains, along with 15 further compounds (analysis of variance [ANOVA], false discovery rate [FDR] ≤ 0.01 ; see Fig. S3B and Table S2). Fifty-four metabolites were present in significantly smaller amounts in the $\Delta dcl2$ strain compared to the WT; at the same time, their production was restored in the $\Delta dcl2+$ strain (ANOVA, FDR ≤ 0.01 ; see Fig. S3B and Table S2). Seventeen of these compounds were tentatively identified or assigned to a compound class by UHPLC-MS, UHPLC-MS/MS, and database mining (Fig. 2B; see also Fig. S3C). Most of these substances were monomeric or dimeric hexaketides of the sorbicillin type (e.g., sorbicillin, sorbicillinol, oxosorbicillinol, epoxysorbicillinol, and bisvertinolone), whereas three glisprenins (I, III, and IV) also were identified. The identification of some of these compounds is outlined below.

Sorbicillin was tentatively identified as a compound eluting at 114.7 s with $[M+H]^+$ m/z 233.118, with two major fragment ions, m/z 95.049 and m/z 165.054, corresponding to bond cleavage on either side of the side chain carbonyl (see Fig. S3C). The ion at m/z 95.049 was diagnostic for all monomeric and dimeric sorbicillin-type compounds containing a hexa-2,4-diene-1-one motif. Fragment ions corresponding to the ion with m/z 165.054 discussed above were important for all monomeric sorbicillin type compounds, and related fragment ions were frequently found with additional loss of CO and/or water, depending on the respective compound structure. The compound eluting at 71.1 s, with $[M+H]^+$ m/z 249.113, was tentatively identified as sorbicillinol based on such fragment ions (see Fig. S3C), and the two compounds at 58.0 s and 94.5 s, both with $[M+H]^+$ m/z 265.207, were suggested to be oxosorbicillinol and epoxysorbicillinol, respectively, based on differences in fragment ions (see Fig. S3C). Five compounds in Fig. 2B gave m/z values which, after database mining, suggested that they were vertinolide or hydroxyvertinolide, hexaketides similar to the sorbicillins but with a lactone head-group instead of the aromatic ring or unsaturated cyclohexanone of sorbicillin-type compounds. In MS/MS, however, the vertinolide-type compounds did not yield fragment ions supporting their structures. Instead, MS/MS data suggested that these compounds were novel dihydrosorbicillinols or oxo/epoxy-dihydrosorbicillinol, respectively.

A large number of dimeric compounds of the sorbicillin-type are known (56), and several share the same molecular formula. These substances are dimerized by several different biosynthetic mechanisms, including Diels-Alder cycloaddition, Michael-type addition reactions, and formation of hemi-ketals. The compound eluting at 129.0 s, with $[M+H]^+$ m/z 513.212 (in accordance with the compound bisvertinolone) gave two



B

Time, Mass to charge ratio	WT	$\Delta ddl2$	$\Delta ddl2+$	Compound
49.3 s, m/z 267.122	26.9 (7.6)	3.7 (0.3)	20.3 (16.9)	dihydrooxosorbicillinol ^a
55.1 s, m/z 233.117	5.7 (1.8)	0.0 (0.0)	8.3 (5.8)	dihydrosorbicillinol ^b
58.0 s, m/z 265.107	39.7 (9.4)	2.6 (2.1)	37.1 (17.7)	oxosorbicillinol
65.4 s, m/z 251.128	272 (121.7)	24.0 (14.2)	269.5 (101.5)	dihydrosorbicillinol ^b
65.7 s, m/z 249.112	77.3 (29.4)	11.2 (6.0)	56.4 (35.2)	sorbicillinol isomer ^c
71.1 s, m/z 249.113	1189.8 (277.0)	124.7 (73.9)	801.6 (612.4)	sorbicillinol
81.2 s, m/z 251.127	130.0 (59.6)	28.0 (9.1)	103.8 (67.7)	2',3'-dihydrosorbicillinol ^b
89.5 s, m/z 251.128	197.9 (58.0)	14.1 (11.3)	345.5 (252.3)	dihydrosorbicillinol ^b
94.5 s, m/z 265.107	79.2 (24.5)	9.5 (6.3)	50.6 (42.1)	epoxysorbicillinol
114.7 s, m/z 233.118	7.4 (4.2)	0.0 (0.0)	4.0 (4.3)	sorbicillin
123.6 s, m/z 753.624	1.8 (0.9)	0.7 (0.3)	29.8 (9.4)	glisoprenin C
125.4 s, m/z 499.233	25.5 (14.3)	0.1 (0.0)	36.8 (38.4)	bisvertinol ^d
125.9 s, m/z 497.216	6.1 (3.2)	0.0 (0.0)	2.6 (1.4)	bisorbicillinol ^e
126.7 s, m/z 501.247	1.0 (0.4)	0.0 (0.0)	3.8 (4.6)	dihydrobisvertinol ^f
129.0 s, m/z 513.212	17.0 (9.6)	0.1 (0.3)	8.3 (8.0)	bisvertinolone
145.2 s, m/z 737.628	4.0 (2.1)	0.4 (0.1)	18.4 (5.2)	glisoprenin D
179.1 s, m/z 703.624	7.0 (1.7)	1.6 (0.4)	37.3 (10.0)	glisoprenin A

FIG 2 UHPLC-MS analysis of cultures of *C. rosea* WT and deletion strains. (A) PCA of UHPLC-MS data from analysis of metabolites produced by *C. rosea* WT and mutant ($\Delta ddl1$, $\Delta ddl2$, $\Delta ddl1+$, and $\Delta ddl2+$) strains. Shaded areas indicate 95% confidence regions. (B) Retention times, mass-to-charge ratios (m/z), extracted-ion chromatogram peak areas, and tentative identification by UHPLC-MS and UHPLC-MS/MS of 17 metabolites produced in significantly smaller amount in $\Delta ddl2$ mutants compared to the WT and restored in the compared $\Delta ddl2+$ strain (ANOVA FDR <0.01). The compound at 125.4 s was comparably underproduced and restored also in the $\Delta ddl1$ strains. Ions are $[M+H]^+$ except for the compound at 55.1 s, which is $[M+H+H_2O]^+$. The peak areas shown are average peak areas $\times 10^{-3}$ with standard deviations in brackets. The heatmap is based on sum-normalized and 10-logarithmized peak areas. Labels in panel A: A, may also be dihydroepoxysorbicillinol; B, proposed to be four different isomers of dihydrosorbicillinol; C, has the same m/z as sorbicillinol but different MS/MS data; D, may also be bisvertinoquinol or isobisvertinol; E, may also be bislongiquinolide or bisorbicillinolide or trichodimerol or trichotetronine; and F, may also be isodihydrobisvertinol.

major fragment ions at m/z 249.111 and m/z 265.107, both $[M+H]^+$, corresponding to the constituting monomeric compounds of bisvertinolone, i.e., sorbicillinol and oxosorbicillinol, respectively (see Fig. S3C). This pattern was observed for all putative dimeric sorbicillin-type compounds, i.e., in UHPLC-MS/MS analyses, these compounds fragmented to yield ions of the presumed constituting monomeric compounds, and related ions after loss of CO and/or water (see Fig. S3C). The formation of these fragment ions is possible for dimeric compounds formed by many different mechanisms, and therefore it was difficult to identify these by MS/MS without access to authentic reference compounds or very detailed information about the MS/MS behavior of these compounds. Therefore, several alternative identities are listed in Fig. 2B for some of the dimeric compounds. The polyhydroxy terpenes glisoprenin A, C, and D were identified based on the m/z of their respective $[M+H]^+$ ions, supported by the m/z of fragment ions (loss of multiple water molecules) detected in UHPLC-MS/MS.

Transcriptome analysis of *Clonostachys rosea* WT and *dcl* deletion strains. To gain insights into the molecular mechanisms associated with the altered phenotypes of *C. rosea* *dcl* deletion strains, transcriptomes of *C. rosea* WT, $\Delta dcl1$, and $\Delta dcl2$ were analyzed by RNA-seq during the interactions with *B. cinerea* and *F. graminearum*. An average of 20.5 million clean reads was obtained for each treatment. Since the sequences contained read pairs from both the interacting species, the reads originating from *C. rosea* or interacting mycohosts were identified by mapping to *C. rosea*, *B. cinerea*, or *F. graminearum* genomes. During the *C. rosea*-*B. cinerea* interaction, 24% of reads, on average, were mapped to *C. rosea* genes, while 58% of reads were assigned to *C. rosea* in the *C. rosea*-*F. graminearum* interaction. Summary data for transcriptome sequencing and mapping are presented in Table S3.

Compared to the *C. rosea* WT, the analysis identified 126 differentially expressed genes (DEGs; 106 upregulated and 20 downregulated) in the $\Delta dcl1$ strain against *B. cinerea*, while this number was much higher against *F. graminearum*, where 897 genes (504 upregulated and 393 downregulated) were differentially expressed (see Table S4). Among these, a majority of genes were uniquely expressed in the respective interaction, since only 32 and 3 genes were commonly upregulated and downregulated, respectively, against both the mycohosts (Fig. 3A). The deletion of *dcl2* affected the expression pattern of a higher number of genes compared to the deletion of *dcl1*. In the $\Delta dcl2$ strain, in comparison to the WT, totals of 1,894 (251 upregulated and 1643 downregulated) and 1,706 (490 upregulated and 1216 downregulated) genes were differentially expressed against *B. cinerea* and *F. graminearum*, respectively (see Table S4). In contrast to the $\Delta dcl1$ strain, where a relatively lower proportion of genes (15.7% against *B. cinerea*; 43.7% against *F. graminearum*) were downregulated, a higher proportion (87% against *B. cinerea*, 73% against *F. graminearum*) of DEGs in the $\Delta dcl2$ strain were downregulated. Among the upregulated genes in the $\Delta dcl2$ strain, 124 genes were commonly upregulated, while 118 genes and 365 genes, respectively, were uniquely upregulated against *B. cinerea* and *F. graminearum*. Among downregulated genes, 669 were common, while 973 and 538 genes, respectively, were unique against *B. cinerea* and *F. graminearum* (Fig. 3B).

The numbers of DEGs overlapping in $\Delta dcl1$ and $\Delta dcl2$ strains during the interactions with a common mycohost were determined (Fig. 3C and D). Among genes that were upregulated in $\Delta dcl1$ or $\Delta dcl2$ strains against *B. cinerea*, 61 were common, while 45 (41%) and 190 (76%) were uniquely upregulated in $\Delta dcl1$ and $\Delta dcl2$ strains, respectively. However, the number of genes downregulated in both mutants against *B. cinerea* was 12. During contact with *F. graminearum*, similar numbers of genes were upregulated in the two mutants (246 in the $\Delta dcl1$ strain, 230 in the $\Delta dcl2$ strain, and 256 in both strains), while the numbers of downregulated genes were greater in the $\Delta dcl2$ strain (93 in the $\Delta dcl1$ strain, 918 in the $\Delta dcl2$ strain, and 296 in both strains) (Fig. 3C and D).

GO enrichment analysis was performed to evaluate which processes were most affected in the *dcl* gene deletion mutants. Our results showed that a higher number of GO

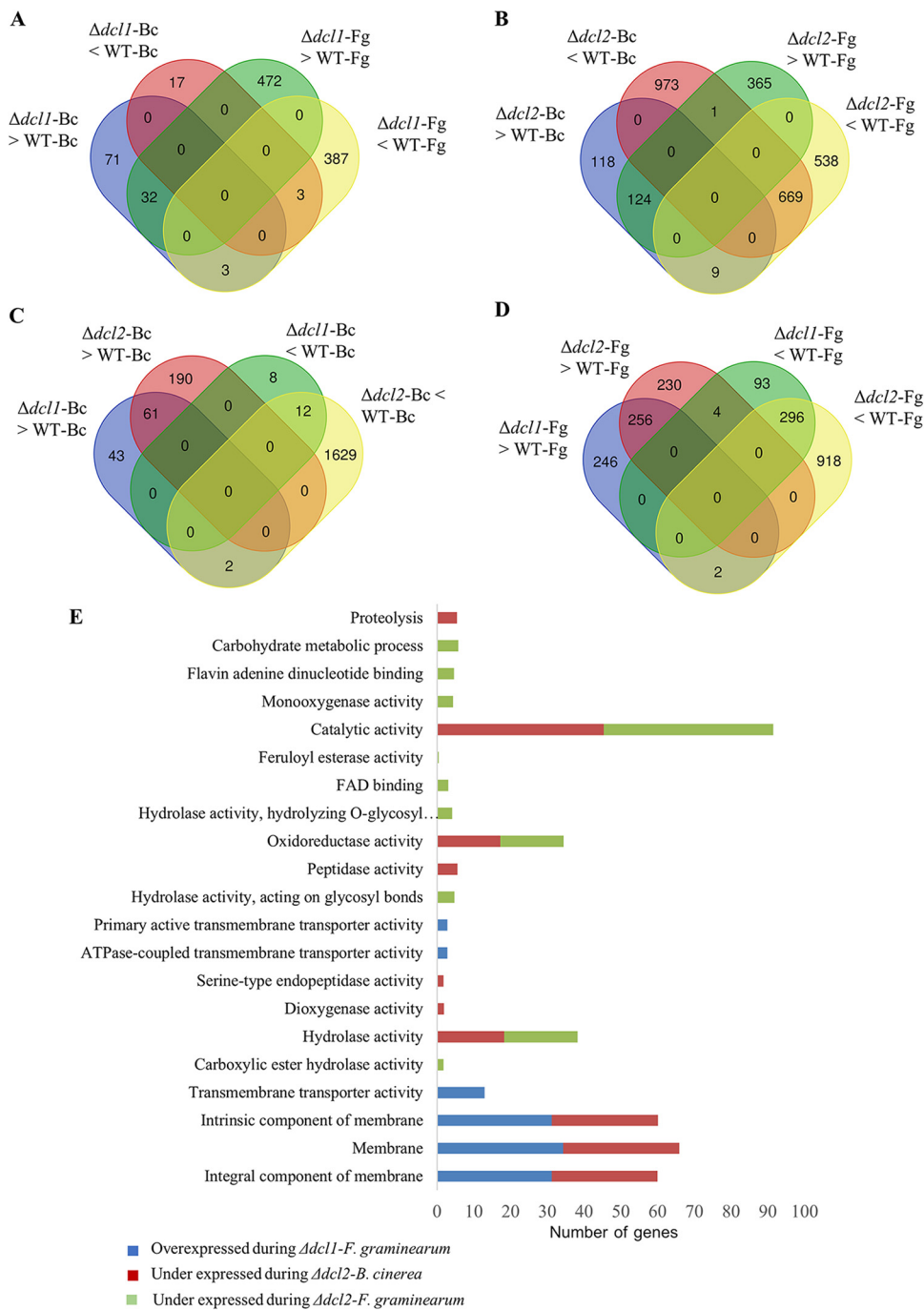


FIG 3 Transcriptome analysis of *C. rosea* WT and *dcl1* and *dcl2* deletion strains during the interactions with *B. cinerea* (Bc) and *F. graminearum* (Fg). (A) Venn diagram showing the common and species-specific DEGs in the $\Delta dcl1$ mutant against *B. cinerea* and *F. graminearum*. (B) Venn diagram showing the common and species-specific DEGs in the $\Delta dcl2$ mutant against *B. cinerea* and *F. graminearum*. (C) Overlap between DEGs in the $\Delta dcl1$ and $\Delta dcl2$ mutants against *B. cinerea*. (D) Overlap between DEGs in $\Delta dcl1$ and $\Delta dcl2$ mutants against *F. graminearum*. (E) Gene Ontology terms enriched in the differentially expressed *C. rosea* genes during the interactions.

terms were significantly enriched in *C. rosea* genes under expressed in the $\Delta dcl2$ strain compared to the whole transcriptome. In the molecular function category, we found that terms such as catalytic activity (GO:0003824), hydrolase activity (GO:0016787), and oxidoreductase activity (GO:0016491) were commonly (against both the mycohosts) enriched ($P \leq 0.05$) among downregulated genes in the $\Delta dcl2$ strain, indicating a role of these

TABLE 1 Number of differentially expressed genes in $\Delta dcl1$ and $\Delta dcl2$ mutants compared to wild-type *C. rosea* during the interaction with *F. graminearum* and *B. cinerea*

Type or function	No. of genes up- or downregulated							
	<i>C. rosea-F. graminearum</i>				<i>C. rosea-B. cinerea</i>			
	$\Delta dcl1$ mutant		$\Delta dcl2$ mutant		$\Delta dcl1$ mutant		$\Delta dcl2$ mutant	
	Up	Down	Up	Down	Up	Down	Up	Down
MFS transporters	26	16	12	64	5	1	6	99
ABC transporters	14	0	10	6	1	0	4	3
SM biosynthesis	45	38	27	99	7	1	13	127
Chitinases	0	0	3	3	1	1	1	3
Transcription factors	24	6	31	28	5	1	17	56
Gene silencing machinery	4	0	4	1	0	0	1	3

genes in mycoparasitism-related functions in *C. rosea* (Fig. 3E). In contrast, other GO terms were only enriched against one of the two mycohosts. This was the case for the protein catabolism terms peptidase activity (GO:0008233) and proteolysis (GO:0006508), specifically enriched during the $\Delta dcl2$ mutant-*B. cinerea* interaction. Carbohydrate metabolism-related terms such as carbohydrate metabolism process (GO:0005975) and hydrolase activity acting on glycosyl bond (GO:0016798) were characteristic for the $\Delta dcl2$ mutant-*F. graminearum* interaction (Fig. 3E).

DCLs regulate genes with a predicted function during fungus-fungus interactions in *Clonostachys rosea*. Since the absence of DCL2 affected the production of secondary metabolites, antagonism, and biocontrol of *C. rosea*, we performed an in-depth analysis of genes with a reported function during interspecific interactions in *C. rosea*, including membrane transporters, enzymes involved in the biosynthesis of secondary metabolites, and hydrolytic enzymes. In addition, the expression pattern of genes coding for transcription factors and various components of the silencing machinery were analyzed. For each of these categories, there were more upregulated genes than downregulated ones in the $\Delta dcl1$ strain. An opposite pattern was evident in the $\Delta dcl2$ strain, where the number of upregulated genes in each category tended to be higher than that of downregulated ones, except for ABC transporters (Table 1; see also Table S5A).

(i) Membrane transporters. Deletion of *dcl2* affected the expression of 161 major facilitator superfamily (MFS) transporters in *C. rosea*. Among these, 12 MFS transporters were upregulated, and 64 were downregulated during interaction with *F. graminearum*, whereas 6 were upregulated, and 99 were downregulated during interaction with *B. cinerea* (Table 1; see also Table S5A). Interestingly, 10 downregulated and 1 upregulated MFS transporters genes in the $\Delta dcl2$ strain showed high sequence similarity ($\geq 48\%$ identity) with MFS transporters previously characterized for their involvement in efflux of secondary metabolites (polyketides, quinones, and polyketide/nonribosomal peptide hybrids) that are important for fungal virulence (Table 2). These included *apdF* (aspyridones efflux protein in *Colletotrichum siamense*), *opS2* (quinone transporter in *Aspergillus udagawae*), *atB* (terreic acid efflux protein in *F. oxysporum*), *FUB11* (fusaric acid efflux pump in *Lachnellula suecica*), *FUBT* (efflux pump involved in export of fusaric acid in *F. culmorum*), *rdc3* (radicol efflux pump in *F. oxysporum*), and *afIT* (aflatoxin efflux pump in *Phialocephala subalpina*) (57–60). Furthermore, a homolog of *FUS6* (fusarin efflux pump *FUS6* in *Colletotrichum fructicola*) was upregulated. However, none of the corresponding gene clusters were present in the genome of *C. rosea*, suggesting that these MFS transporters constitute resistance proteins activated as a defense against harmful, hitherto-unknown, secondary metabolites. Moreover, 22 MFS transporter genes were previously reported to be induced in *C. rosea* during the interactions with *B. cinerea* and *F. graminearum* (49). Nine of these MFS transporter genes were significantly downregulated in the $\Delta dcl2$ strain during the interactions with *B. cinerea* or *F. graminearum* (Table 2). In summary the $\Delta dcl2$ mutant showed downregulation

TABLE 2 Differential expression patterns of selected genes in *C. rosea* $\Delta dcl1$ and $\Delta dcl2$ mutant strains during interactions with *B. cinerea* or *F. graminearum* compared to those of WT *C. rosea*

Gene ID	Log ₂ FC expression ^a				Comment(s)
	$\Delta dcl1$ (Bc)	$\Delta dcl1$ (Fg)	$\Delta dcl2$ (Bc)	$\Delta dcl2$ (Fg)	
Differentially expressed MFS transporter genes identical to previously characterized MFS transporters					
CRV2G00017900	-0.36	-1.94	0.23	-5.05	<i>mfs212</i> (ID 50% with <i>apdF</i> [PKS-NRPS transport])
CRV2G00017824	0.36	-0.68	0.21	-1.54	<i>mfs</i> (ID 48% OpS2 [Quinone transport])
CRV2G00015530	-0.21	-1.89	0.09	-2.28	<i>mfs</i> (ID 59% with atB [terreic acid transport])
CRV2G00015418	0.02	-1.61	-1.09	-1.56	<i>mfs</i> (ID 60% with FUB11 [polyketide transport])
CRV2G00004817	0.53	-1.6	-4.04	-2.92	<i>mfs506</i> (ID 57% with FUBT [polyketide transport])
CRV2G00002357	-0.4	-1.26	-1.69	-1.96	<i>mfs533</i> (ID 70% with rdc3 [polyketide transport])
CRV2G00016200	0.12	-0.69	-2.31	-2.18	<i>mfs530</i> (ID 60% with rdc3 [polyketide transport])
CRV2G00004939	0.22	-1.76	-2.09	-3.04	<i>mfs534</i> (ID 80% with rdc3 [polyketide transport])
CRV2G00019617	1.94	4.06	1.59	3	<i>mfs595</i> (ID 77% with FUS6 [polyketide transport])
CRV2G00011170	0.95	0.17	0.14	-3.32	<i>mfs602</i> (ID 60% with aflT [polyketide transport])
CRV2G00005334	0.05	-5.44	-4.55	-5.94	<i>mfs589</i> (ID 70% with aflT [polyketide transport])
Reduced expression of MFS transporters that were induced in <i>C. rosea</i> against <i>B. cinerea</i> or <i>F. graminearum</i>					
CRV2G00004685	0.32	-0.79	0.62	-1.57	<i>mfs464</i>
CRV2G00005389	-0.81	-0.75	-1.79	-1.38	<i>mfs271</i>
CRV2G00018263	-0.37	-0.79	-0.74	-2.14	<i>mfs524</i>
CRV2G00011170	-0.03	-1.18	0.14	-3.32	<i>mfs602</i>
CRV2G00012180	1.12	-2.65	-1.45	-2.9	<i>mfs166</i>
CRV2G00015972	-0.06	-2.26	-1.77	-2.3	<i>mfs205</i>
CRV2G00004853	0.45	-1.45	-2.37	-2.27	<i>mfs104</i>
CRV2G00004939	0.22	-1.76	-2.09	-3.04	<i>mfs534</i>
CRV2G00018885	-0.39	-1.22	-3.55	-2.63	<i>mfs24</i>
Differentially expressed polyketide and nonribosomal peptide synthetase genes					
CRV2G00011222	-0.67	0.01	0.03	-1.88	<i>pks14</i>
CRV2G00013582	0	-1.43	-0.03	-1.61	<i>pks23</i>
CRV2G00015413	0.75	-2.28	-1.86	-2.96	<i>pks12</i>
CRV2G00015415	1.09	-2.7	-3.22	-3.15	<i>pks2</i>
CRV2G00018696	-0.92	-0.63	-0.13	-4.97	<i>pks6</i>
CRV2G00018222	0.03	-1.43	-2.43	-1.79	<i>pks22</i>
CRV2G00004952	0.11	1.88	0.74	1.54	<i>nrps</i>
CRV2G00005605	0.65	2.73	1.95	2.33	<i>nrps</i>
CRV2G00012656	0.18	1.82	1.95	2.17	<i>nrps16</i>
CRV2G00015275	-0.15	-0.7	0.76	-2.06	<i>nrps</i>
CRV2G00016915	0.67	-1.91	-3.07	-3.17	<i>nrps</i>
CRV2G00014896	0.25	1.44	1.26	1.68	<i>nrps9</i>
CRV2G00005211	0.26	-1.62	-3.74	-2.3	Indole
CRV2G00002084	4.33	0.12	5.24	-0.84	Terpene
Differentially expressed transcription factor genes identical to previously characterized transcription factors					
CRV2G00004759	-0.69	-0.32	-1.75	-1.02	ID 60% with FGR27
CRV2G00006707	-0.01	-0.9	-1.62	-1.31	ID 73% with CCAAT-binding subunit HAP3
CRV2G00015419	0.29	-0.95	-2.22	-1.73	ID 53% with sorbicillin regulator YPR2
CRV2G00011734	0.32	1.81	0.56	1.41	ID 79% with <i>abaA</i>
CRV2G00011385	0.19	-0.46	2.58	1.16	ID 57% with CTF1
CRV2G00016352	0.73	1.51	0.47	1.3	ID 65–70% SUC1
CRV2G00019080	1.98	2.1	1.16	1.5	ID 65% with SUC1
CRV2G00019116	0.9	2.32	1.01	2.2	ID 70% SUC1
CRV2G00016935	-0.74	-0.22	-1.69	-0.7	ID 69% with <i>prt7</i>
CRV2G00018531	-0.21	-0.48	-2.12	-1.35	ID 61% with sterol uptake control 2
CRV2G00019093	-0.38	0.43	-1.5	-0.14	ID 60% with GAL4
Differentially expressed chitinases and <i>N</i> -acetylhexosaminidase genes					
CRV2G00001280	-0.08	-0.85	-3	-1.67	Chitinase <i>ech42</i>
CRV2G00003425	-0.3	-1.54	-3.6	-3.2	Chitinase <i>ech37</i>
CRV2G00018858	-0.01	-0.06	-1.9	-1.82	Chitinase <i>chia5</i>
CRV2G00017631	-0.07	0.16	0.62	2.51	Chitinase
CRV2G00006887	0.82	2.18	0.92	1.75	Chitinase <i>ech58</i>
CRV2G00011101	-0.3	-0.13	2.25	2.1	Chitinase <i>chic1</i>

(Continued on next page)

TABLE 2 (Continued)

Gene ID	Log ₂ FC expression ^a				Comment(s)
	$\Delta dcl1$ (Bc)	$\Delta dcl1$ (Fg)	$\Delta dcl2$ (Bc)	$\Delta dcl2$ (Fg)	
CRV2G00002927	-0.21	-0.42	-1.76	-0.78	NAG
CRV2G00012950	-0.14	-0.43	-2.5	-2.26	NAG
Differentially expressed genes associated with gene silencing machinery					
CRV2G00000975	0.2	0.1	1.2	1.9	Argonaute2-like
CRV2G00016556	0.2	2.1	0.4	1.3	Chromatin remodeling protein
CRV2G00012165	0.2	4	-0.4	4.3	Histone deacetylase
CRV2G00007951	0.4	0.4	1	1.6	Histone deacetylase
CRV2G00006603	0.9	2.3	2.4	2.3	RNA helicase
CRV2G00007159	0.6	1.6	0.5	1	RNA helicase
CRV2G00001612	-0.6	0.1	-1.6	-1.8	RNA helicase
CRV2G00012613	-0.7	0.9	-2.4	0.1	RNA helicase
CRV2G00009762	0	0.9	-1.7	-0.6	RNA-directed RNA polymerase

^aSignificant differences are indicated in boldface letters. FDR < 0.05 in combination with a log₂ fold change (log₂FC) of >1.5 or <-1.5 was considered to define differentially expressed genes. Bc, *B. cinerea*; Fc, *F. graminearum*.

of transporters with predicted function in secondary metabolite export and putative detoxification.

In contrast to the expression pattern of MFS transporters, a higher number of ATP-binding cassette (ABC) transporter genes was upregulated in both the deletion strains, but specifically against *F. graminearum*, where 14 and 10 genes, respectively, were upregulated in the $\Delta dcl1$ or $\Delta dcl2$ mutant (Table 1). Of 19 ABC transporters that were differentially regulated in $\Delta dcl2$, 5 upregulated and 1 downregulated belonged to the multidrug resistance protein (MDR) subfamily, 3 downregulated and 1 upregulated belonged to the multidrug resistance-associated protein (MRP) subfamily, and 4 upregulated and 1 downregulated belonged to pleiotropic drug resistance protein (PDR) subfamily (see Table S5A).

(ii) Secondary metabolite biosynthetic genes. Genes associated with secondary metabolite production are often arranged in biosynthetic gene clusters (BGCs) that consist of genes coding for core enzymes typically nonribosomal peptide synthetase (NRPS), polyketide synthase (PKS), or terpene cyclase, together with genes coding for additional proteins, including modifying enzymes, transporters, and transcription factors (61). We used antiSMASH to predict the biosynthetic gene clusters in *C. rosea* and identified 33 NRPS BGCs, 29 PKS BGCs, 7 BGCs for terpenes and 7 BGCs for NRPS-PKS hybrids, and 1 BGC for indole and betalactone biosynthesis.

Gene expression analysis of both $\Delta dcl1$ and $\Delta dcl2$ mutants identified a total of 230 DEGs predicted to be part of BGCs involved in secondary metabolite biosynthesis. Among the BGCs, the core biosynthetic genes in eight NRPS, five PKS, one terpene, and one indole BGCs were differentially regulated in the $\Delta dcl2$ mutant against *B. cinerea* or *F. graminearum* (Table 2; see also Table S5A). Interestingly, NRPS and PKS BGC core genes showed expression patterns opposite to each other since NRPS BGC core genes were mostly upregulated in the $\Delta dcl2$ mutant, whereas PKS BGC core genes were downregulated (Table 2). Among the downregulated core genes of PKS BGCs were the three PKS genes *pks22*, *pks2*, and *pks12*, reported to be part of previously identified BGCs responsible for the production of clonorosein and sorbicillin in *C. rosea* and *T. reesei*, respectively (Fig. 4) (50, 62). Sorbicillin is the precursor for sorbicillinol, which is in turn necessary for other sorbicillinoid compounds (63), explaining the low production of these substances by the $\Delta dcl2$ mutant.

(iii) Transcription factors. The transcriptome analysis further identified 128 differentially expressed genes predicted to encode transcription factors in the $\Delta dcl1$ and $\Delta dcl2$ strains (Table 1; see also Table S5A). We identified 11 transcription factors genes that were differentially expressed in the $\Delta dcl1$ strain and/or in the $\Delta dcl2$ strain and showed >50% sequence identity with genes previously characterized for their role as transcriptional regulators. CRV2G00011734 was upregulated in the $\Delta dcl1$ strain and

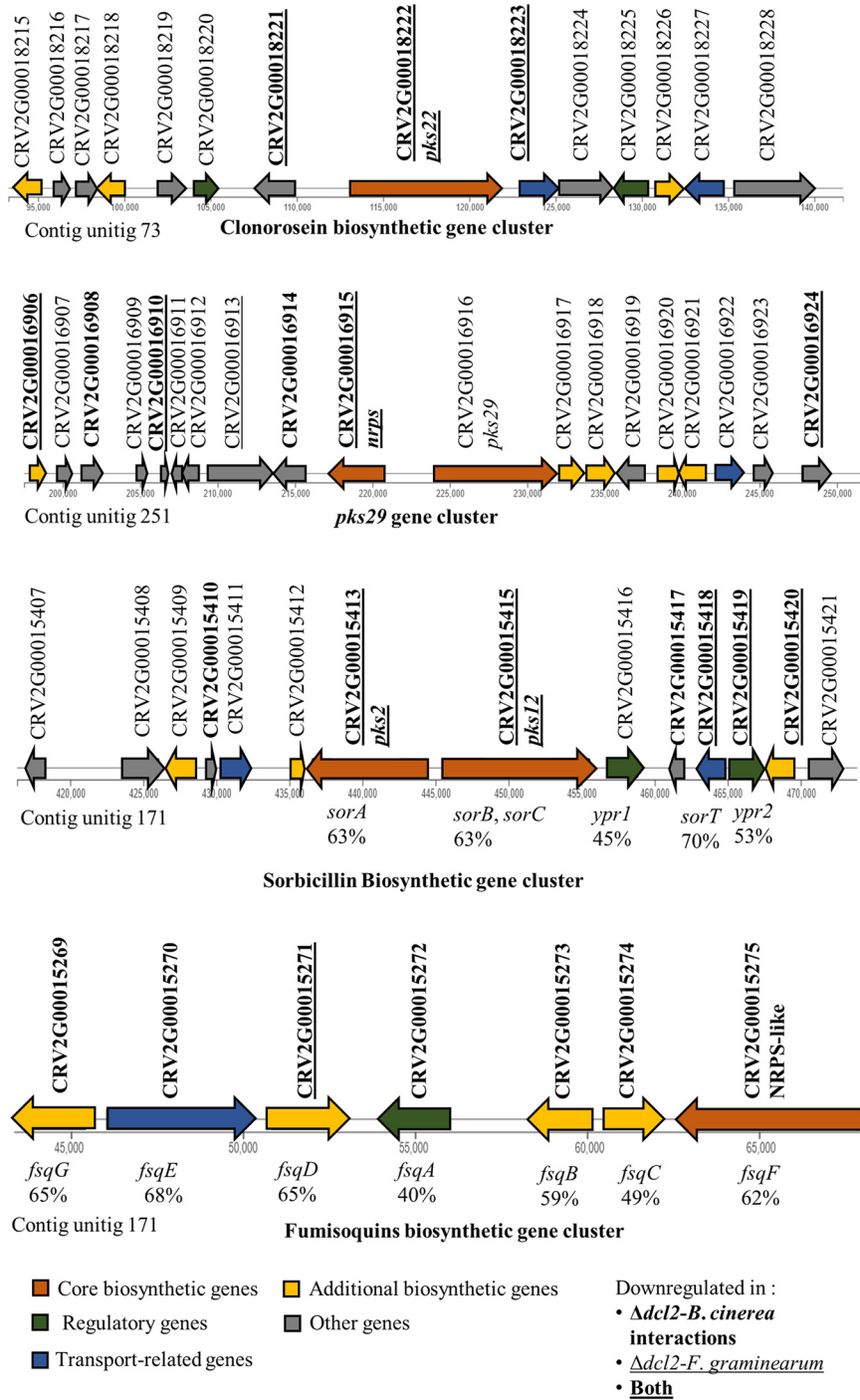


FIG 4 Expression of predicted *C. rosea* gene clusters of clonorsein, *pks29*, sorbicillin, and fumisoquins. Gene IDs in boldface letters indicate downregulated genes during $\Delta dcl2$ mutant-*B. cinerea* interactions. Underlining indicates downregulated genes during $\Delta dcl2$ mutant-*F. graminearum* interactions. Boldfacing and underlining indicates genes that were downregulated against both mycohosts. The gene names for the sorbicillin and fumisoquin gene clusters were assigned by comparison to *Trichoderma reesei* and *Aspergillus fumigatus*, respectively (63, 73). A minimum query coverage of 80% was required in the comparison, and the maximum E value was fixed at 1×10^7 .

showed identity with the conidiophore development regulator gene *abaA* (64, 65), whereas CRV2G00016352, CRV2G00019080, and CRV2G00019116, also upregulated, showed identity with the sucrose metabolic gene *suc1*, shown to be associated with mitotic and meiotic cell division in fission yeast (66). The genes CRV2G00004759, CRV2G00006707,

and CRV2G00015419, downregulated in the $\Delta dcl2$ mutant, showed identity with transcription factor genes *fgf27*, *hap3*, and *ypr2*, shown to be involved in regulating growth and secondary metabolite production (62, 67, 68) (Table 2). In summary, the Dicer-dependent control of transcription factor gene expression was to a large degree mycohost specific, with no transcription factors differentially expressed against both mycohosts in the $\Delta dcl2$ mutant. Moreover, among the identified transcription factors, there were many homologs of genes known to have a role in regulating secondary metabolism and growth.

(iv) Glycosyl hydrolase families 18 and 20. The *C. rosea* genome contains 13 genes coding for enzymes with predicted chitinase (glycoside hydrolase family 18 [GH18]) activity (44), 6 of which were differentially regulated in the $\Delta dcl2$ mutant against *B. cinerea* or *F. graminearum* (see Table S5A). Among these, CRV2G00001280 (*ech42*), CRV2G00003425 (*ech37*), and CRV2G00018858 (*chiA5*) were downregulated against both the mycohosts, while CRV2G00017631, CRV2G00006887 (*ech58*), and CRV2G00011101 (*chiC1*) were upregulated against both the mycohosts (Table 2). Furthermore, the *C. rosea* genome contains two genes (CRV2G00002927 and CRV2G00012950) coding for predicted *N*-acetylhexosaminidases (NAG; GH20), the expression of which was downregulated in the $\Delta dcl2$ strain against *B. cinerea* (both genes) and *F. graminearum* (only CRV2G00012950). In summary, many glycoside hydrolases with a known role in degrading mycohost cell walls were downregulated in the $\Delta dcl2$ mutant after contact with the mycohosts.

(v) Genes associated with gene silencing machinery. To investigate an effect of *dcl1* and *dcl2* deletions on various protein components involved in the gene silencing machinery through chromatin modification in *C. rosea*, Blast2GO was used to identify genes encoding RNA helicases, chromatin remodeling proteins, histone deacetylases, and histone methyltransferases. We identified 118 genes (excluding DCL, AGO, and RDR), including 67, 23, 18, and 3 genes coding for RNA helicases, chromatin remodeling proteins, histone deacetylases, and histone methyltransferases, respectively (see Table S5B). Deletion of *dcl1* did not cause differential expression in the $\Delta dcl1$ mutant-*B. cinerea* interaction, whereas during contact with *F. graminearum* we detected upregulation of two RNA helicase genes (CRV2G00006603 and CRV2G00007159), one gene coding for a chromatin remodeling protein (CRV2G00016556) and a histone deacetylase gene (CRV2G00012172), while one histone deacetylase gene (CRV2G00012172) was downregulated (Table 2). During the $\Delta dcl2$ -*B. cinerea* interaction, one RNA helicase gene (CRV2G00006603) was upregulated, and two RNA helicases (CRV2G00001612 and CRV2G00012613), as well as an RNA-directed RNA polymerase (CRV2G00009762) were downregulated. Conversely, during the $\Delta dcl2$ mutant-*F. graminearum* interaction, two histone deacetylases (CRV2G00012165 and CRV2G00007951), one RNA helicase gene (CRV2G00006603), and one gene coding for an Argonaute protein (CRV2G00000975) were upregulated, whereas one RNA helicase (CRV2G00001612) gene was downregulated (Table 2). In summary, many genes involved in chromatin modification and gene silencing are affected by the deletion of the *dcl* enzymes, particularly *dcl2*. Most of these, including an Argonaute protein, are upregulated, possibly due to the diminished presence of regulating sRNAs in the mutants.

Analysis of sRNAs characteristics in the *Clonostachys rosea* WT and the *dcl* deletion strains. To investigate the effect of sRNAs on transcriptional regulation in *C. rosea*, sRNA libraries from *C. rosea* WT, $\Delta dcl1$, and $\Delta dcl2$ strains interacting with *B. cinerea* or *F. graminearum* were sequenced. The sequencing produced 16 million reads per sample on average. Between 61 and 72% of these read pairs were composed of nonstructural RNAs, including rRNA, tRNA, snoRNA, and snRNA, and were excluded from the further analysis. The remaining subset of reads that were 18 to 32 nucleotides (nt) long were used for alignment to the genomes of *C. rosea*, *B. cinerea*, and *F. graminearum*. A summary of sRNA characteristics and their alignment to the respective genome is presented in Table S6A in the supplemental material. sRNAs mapping exclusively to the *C. rosea*, *B. cinerea*, or *F. graminearum* genome (unique sRNAs) were selected for further analysis. On average 42% of sRNA reads from *C. rosea*-*B. cinerea* interactions were aligned uniquely to one of the two organisms, while this percentage was only 18% for *C. rosea*-*F. graminearum* interactions. This is plausible because

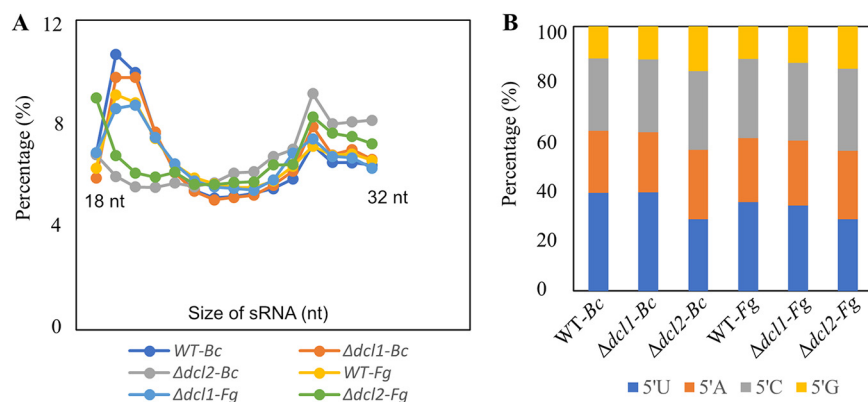


FIG 5 sRNA characteristics in *C. rosea* wild-type (WT) and *dcl* deletion strains. (A and B) Length distribution (A) and 5' end nucleotide preference (B) of nonstructural sRNAs produced by *C. rosea* WT and *dcl* deletion strains during the interactions with *F. graminearum* (Fg) and *B. cinerea* (Bc). Only sRNAs between 18 and 32 nt in length are considered.

C. rosea is evolutionarily closer to *F. graminearum* (both belong to order *Hypocreales*) than to *B. cinerea*.

We compared the characteristics of sRNAs produced in the $\Delta dcl1$ and $\Delta dcl2$ mutants to those of the WT. The analysis of length distribution showed a significant reduction in sRNAs with a size of 19 to 22 nt in the $\Delta dcl2$ compared to the WT, while no difference in sRNA abundance was found between the $\Delta dcl1$ and WT strains (Fig. 5A). The analysis of the 5' terminal nucleotide composition showed a reduced proportion of reads (27%) with 5' end uracil (5'-U) in the $\Delta dcl2$ strain, compared to a 32 to 37% proportion of reads with 5'-U from the WT and $\Delta dcl1$ strains (Fig. 5B). The origin of sRNAs was not significantly affected by the deletion of *dcl* genes, with most reads mapping to coding sequences (CDSs; 49%), followed by intergenic regions (25%), promoters (12.3%), 3' untranslated regions (UTRs) (8%), introns (4%), and 5' UTRs (1.5%). A higher proportion (83.5%) of sRNAs was mapped with the sense orientation, rather than the antisense one, similar to what was reported in previous studies in *F. graminearum* and *T. atroviride* (20, 69), and this might be due to by-products of mRNA degradation. However, the relative proportion of sRNAs mapping to the antisense direction was reduced from an average of 17.5% during WT-*B. cinerea* interaction to 14.3% during $\Delta dcl2$ strain-*B. cinerea* interaction (see Table S6A).

(i) miRNA prediction in *Clonostachys rosea*. Mirdeep2 analysis predicted 61 miRNAs in *C. rosea* with lengths between 18 and 25 nt, and they were named cro-mir's. These miRNAs originated from a variety of positions in the genome including promoters, introns, CDSs, and UTRs, but mainly (28 of 61) from intergenic regions (see Table S6B). The expression of 15 cro-mir's was common against both mycohosts, whereas 29 and 17 cro-mir's were expressed specifically during interaction with *B. cinerea* or *F. graminearum*, respectively (see Table S6B). Interestingly, no cro-mir was found to be differentially expressed in the $\Delta dcl1$ mutant during the interspecific interactions, while 11 cro-mir's were significantly downregulated in the $\Delta dcl2$ mutant during interaction with both mycohosts (Table 3). This downregulation was confirmed through stem-loop RT-qPCR (Table 3). A single miRNA (cro-mir-23) was identified as upregulated in the $\Delta dcl2$ mutant in the RNA-seq analysis but downregulated according to stem-loop RT-qPCR.

(ii) Identification of cro-miRNAs endogenous gene targets. Twenty-one putative endogenous gene targets were identified for the 11 cro-mir's downregulated in $\Delta dcl2$ (Table 4). Eight gene targets were commonly upregulated in $\Delta dcl2$ during the interaction with *B. cinerea* and *F. graminearum*, while seven and six gene targets were uniquely upregulated during the interactions with *B. cinerea* and *F. graminearum*, respectively (Table 4). Among the predicted gene targets, several had putative regulatory roles: CRV2G00015277, CRV2G00002266, and CRV2G00002043 were predicted to

TABLE 3 Differentially expressed cro-mir's, their lengths, and their loci of origin^a

miRNA identifier	Sequence (5'–3')	Length (nt)	Log ₂ FC				Origin
			RNA-seq		Stem-loop RT-qPCR		
			$\Delta dcl2$ (Bc)	$\Delta dcl2$ (Fg)	$\Delta dcl2$ (Bc)	$\Delta dcl2$ (Fg)	
cro-mir-1	TAGAATTCGGGGTAGAAT	18	−7.90	−7.15	−8.22	−9.43	Intergenic
cro-mir-2	TAGAATTCGGGGTAGAATG	19	−8.70	−8.23	−3.33	−10.94	Intergenic
cro-mir-3	TTAGCCTCGAGACTTTGCA	19	−8.28	−7.23	−5.85	−2.16	3' UTR
cro-mir-4	TCAGCCTCGAGACTTTGCC	19	−8.47	−6.25	−2.18	−2.92	3' UTR
cro-mir-5	TTGCAATGATTTGCATTTCCGC	21	−3.52	−2.61	−3.54	−1.31	Intergenic
cro-mir-6	TAGGACTCGAGTAGTTATAAC	21	−4.39	−4.70	−2.05	−1.75	Intergenic
cro-mir-9	TCGGACGTATATTGACTACTC	21	−3.88	−3.22	−2.87	−2.71	Promoter
cro-mir-10	TCGGTGGGATGTTTGAGACT	20	−3.80	−2.59	−3.43	−3.21	Promoter
cro-mir-11	TAGAGTTTTTGAGATGCT	19	−5.22	−4.68	−5.31	−3.05	Promoter
cro-mir-13	TTCTTCCTTGATGCGTCCC	19	−7.92	−7.74	−5.64	−6.07	3' UTR
cro-mir-23	CTGGCAGGTATGGTCGTAGATG	22	+2.68	+2.18	−2.09	−3.10	Intergenic
cro-mir-36	TCAAACACAATTAGCGGTC	19	−7.30	−6.21	−4.26	−3.50	Intergenic

^ant, nucleotides; UTR, untranslated region; Bc, *B. cinerea*; Fc, *F. graminearum*.

encode putative transcription factors, CRV2G00001868 encodes an ATP-dependent helicase, while CRV2G00004332 and CRV2G00008014 encode a GTP binding protein and a GTPase with a putative role in signal transduction. Moreover, CRV2G00014914 was located in a secondary metabolite gene cluster and might have a role in regulating secondary metabolism (Table 4).

TABLE 4 Endogenous putative gene targets in *C. rosea*, their expression patterns, and their predicted functions

miRNA identifier	Gene target	Expression log ₂ FC ^a		Target gene family	Characterized/putative function
		$\Delta dcl2$ (Bc)	$\Delta dcl2$ (Fg)		
cro-mir-3	CRV2G00002264	1.08	1.42	Serine/threonine-protein kinase (Gin4)	Septin ring assembly, intracellular signal transduction
cro-mir-5	CRV2G00013335	1.39	1.25	Unknown	Unknown function
cro-mir-5	CRV2G00015277	2.54	3.52	Transcription factor	60S ribosome biogenesis
cro-mir-10	CRV2G00015277	2.54	3.52	Transcription factor	60S ribosome biogenesis
cro-mir-11	CRV2G00015277	2.54	3.52	Transcription factor	60S ribosome biogenesis
cro-mir-13	CRV2G00001868	1.95	2.72	Helicase	Chromatin remodeling
	CRV2G00002266	1.81	1.98	Transcriptional regulator <i>prz1</i>	Regulates the expression of the Pmc1 ATPase Ca ²⁺ pump
cro-mir-36	CRV2G00013380	2.42	3.36	ATPase	ATPase activity
	CRV2G00005499	1.38	1.8	Unknown	Unknown function
	CRV2G00000111	1.95	2.69	Unknown	Unknown function
	CRV2G00014914	1.21	0.82	Oxidation-reduction process	Part of secondary metabolite BGC
cro-mir-1	CRV2G00003756	1.06	0.89	tRNA ligase	Protein biosynthesis
cro-mir-2	CRV2G00003756	1.06	0.89	tRNA ligase	Protein biosynthesis
cro-mir-3	CRV2G00008014	1.12	0.23	GTPase-activating protein 2	Signal transduction
cro-mir-6	CRV2G00002043	1.12	0.99	Transcription factor	Regulation
cro-mir-3	CRV2G00009307	1.26	0.81	Sterol O-acyltransferase 2	Cholesterol metabolic process
cro-mir-11	CRV2G00009307	1.26	0.81	Sterol O-acyltransferase 2	Cholesterol metabolic process
cro-mir-3	CRV2G00011242	1.26	0.75	Oxidoreductase	Oxidation-reduction
cro-mir-4	CRV2G00011242	1.26	0.75	Oxidoreductase	Oxidation-reduction
cro-mir-13	CRV2G00004332	1.06	0.43	GTP-binding protein	Ribosome biogenesis
cro-mir-1	CRV2G00005300	0.69	1.38	Unknown	Unknown function
cro-mir-4	CRV2G00004339	0.48	1.03	SNF2 RNA helicase	Chromatin remodeling
cro-mir-9	CRV2G00004339	0.48	1.03	SNF2 RNA helicase	Chromatin remodeling
cro-mir-10	CRV2G00004339	0.48	1.03	SNF2 RNA helicase	Chromatin remodeling
cro-mir-11	CRV2G00000903	0.82	1.03	Unknown	Unknown function
cro-mir-36	CRV2G00000903	0.82	1.03	Unknown	Unknown function
cro-mir-10	CRV2G00011823	0.93	1.21	Choline-sulfatase	Hydrolase activity
cro-mir-36	CRV2G00011823	0.93	1.21	Choline-sulfatase	Hydrolase activity
cro-mir-4	CRV2G00012062	−0.18	1.09	Unknown	Unknown function
cro-mir-13	CRV2G00012781	0.3	1.01	Unknown	Unknown function

^aUpregulated (FDR < 0.05 in combination with log₂FC > 1) gene targets are highlighted in boldface. Bc, *B. cinerea*; Fc, *F. graminearum*.

(iii) Cross-species gene target identification. Using the criteria described for the endogenous gene target prediction, we identified 513 putative cross-species gene targets in *B. cinerea* (see Table S6C). Among these, the seven genes *bcpls1*, *bcpka1*, *bcnoxA*, *bcste11*, *bccap9*, *bccrh1*, and *bcchsIV* were previously characterized for their role in growth and development, proteolysis, and consequently virulence (Table 5). Moreover, a gene encoding a *B. cinerea* homolog of SSAMS2 (BCIN_08g03180) was also among the putative targets, and this gene encodes a GATA transcription factor required for appressoria formation and chromosome segregation in *Sclerotinia sclerotiorum* (70). In addition, *bcnog1* and *bchts1* encoding proteins putatively involved in ribosome biogenesis, and *bcphy2* and *bchhk1* encoding signal transduction proteins were also identified as putative targets. Finally, three genes coding for a protein with a putative role in chitin recognition (*bcgo1*), chromatin remodeling (*bcyta7*), and intracellular trafficking and secretion (*bcvac8*) were also identified (Table 5).

Thirty-five cross-species gene targets were predicted in *F. graminearum* as well. We identified three previously characterized virulence factors (FGSG_07067, FGSG_02083, and FGSG_00376) as putative targets of *cro-mir-3*, *cro-mir-4*, and *cro-mir-5*, respectively (Table 5). In addition, three membrane transporter genes (FGSG_13747, FGSG_13747, and FGSG_13747) and two genes coding for proteins with a putative role in intracellular trafficking and secretion (FGSG_09686 and FGSG_09686) were identified as putative targets (Table 5). In summary, several mycohost genes with a role in virulence, intracellular trafficking, secretion, and regulation were identified as putative targets of *C. rosea dcl2*-dependent miRNAs.

***Botrytis cinerea* and *Fusarium graminearum* responded differently toward *Clonostachys rosea* WT and *dcl* deletion strains.** Transcriptome analysis of *B. cinerea* and *F. graminearum* was performed to investigate whether the deletion of *dcl* genes affects their response mechanism to *C. rosea*. Read pairs unique to *B. cinerea* from the *C. rosea*-*B. cinerea* interaction and unique to *F. graminearum* from the *C. rosea*-*F. graminearum* interaction were used in the analysis. From the total number of read pairs that originated from the *C. rosea*-*B. cinerea* or *C. rosea*-*F. graminearum* interactions, 25 and 23% reads were uniquely assigned to *B. cinerea* and *F. graminearum*, respectively (see Table S3).

In comparison to the WT-*B. cinerea* interaction, 24 genes (21 upregulated and 3 downregulated) were differentially expressed in *B. cinerea* during the $\Delta dcl1$ mutant-*B. cinerea* interaction. However, 721 genes were found to be differentially regulated (655 upregulated and 66 downregulated) in the interaction with the $\Delta dcl2$ mutant (Fig. 6A; see also Table S6C). The 21 *B. cinerea* genes that were upregulated against the $\Delta dcl1$ strain were also upregulated against the $\Delta dcl2$ strain (Fig. 6A). We specifically investigated genes coding for hydrolytic enzymes, transcription factors, membrane transporters, known virulence factors, RNA silencing component proteins, and genes that are part of secondary metabolite BGCs. During $\Delta dcl1$ mutant-*B. cinerea* interaction, one gene (BCIN_14g03930) coding for a known virulence factor and two genes coding for MFS transporters were upregulated, while two genes that were part of secondary metabolite BGCs were downregulated in *B. cinerea*. Deletion of *dcl2* induces increased expression of 12 genes previously characterized for their role in growth and development, virulence, and pathogenesis in *B. cinerea*. Among the other genes, we detected the upregulation of GTPases, kinases, chitinases, squalene monooxygenases, and genes involved in chitin synthesis and chitin recognition (Table 6).

The other differentially expressed genes did not have a characterized functional role, but a function was predicted for some of them. In particular, among the genes upregulated during the $\Delta dcl2$ mutant-*B. cinerea* interaction, we detected 49 putatively coding for hydrolytic enzymes, 24 located in putative secondary metabolite BGCs, 22 transcription factors, 17 genes involved in RNA silencing, 15 protein kinases, and 13 MFS transporters (see Table S6C). GO enrichment analysis of upregulated genes during the $\Delta dcl2$ mutant-*B. cinerea* interactions identified terms for metabolic processes, including gene expression (GO:0010467), cellular component organization or biogenesis (GO:0071840), and RNA processing (GO:0006396) (Fig. 6B). However, GO terms oxidoreductase

TABLE 5 Most important cross-species putative gene targets in *B. cinerea* and *F. graminearum*, their expression pattern and putative function

miRNA identifier	Gene target transcript ID	Locus ID (gene name)	Expression (log ₂ FC)	Target gene family	Characterized or putative function
<i>Botrytis cinerea</i>					
cro-mir-1, cro-mir-2, and cro-mir-6	XM_024690817	Bcin_01g09230 (<i>bcphy2</i>)	3.53	Protein kinase	Signal transduction
cro-mir-9	XM_024690817	Bcin_05g05430	3.38	Phospholipid methyltransferase	Lipid metabolic process (membrane lipid biogenesis)
cro-mir-13	XM_001553702	Bcin_02g04090	2.9	Fungal 1,3(4)- β -D-glucanases	Glucan catabolic process
cro-mir-13 and cro-mir-2	XM_001547426	Bcin_01g00360 (<i>bcerg1</i>)	2.74	Squalene monooxygenase	Sterol biosynthetic process
cro-mir-4	XM_001557947	Bcin_12g00180 (<i>bccap9</i>)	2.69	Aspartic proteases of fungal origin	Proteolysis, induced during infection
cro-mir-5	XM_001557734	Bcin_04g06150	2.29	Cyclase (Lanc-like super family)	Biosynthesis of lantibiotics
cro-mir-1 and cro-mir-2	XM_024693876	Bcin_07g01580 (<i>bcnog1</i>)	2.27	GTP-binding protein	Ribosomal large subunit biogenesis
cro-mir-4	XM_024693364	Bcin_06g01930 (<i>bcgo1</i>)	1.87	Chitin binding	Chitin recognition
cro-mir-5	XM_001561274	Bcin_01g06010 (<i>bccrth1</i>)	1.83	Glycosylphosphatidylinositol-glucanosyltransferase	Fungal cell wall biosynthesis
cro-mir-5	XM_024691832	Bcin_03g02630 (<i>bcste11</i>)	1.81	Protein kinase	Signal transduction, virulence
cro-mir-36	XM_024691483	Bcin_02g06930	1.67	1,3- β -D-Glucan synthase	Glucan biosynthesis
cro-mir-36	XM_001558808	BCIN_02g02410	1.61	Glycosyl hydrolase	Fungal-type cell wall polysaccharide metabolic process
cro-mir-11	XM_001551241	BCIN_14g02820	1.57	β -Glucan synthesis-associated protein	Fungal cell wall biosynthesis
cro-mir-11	XM_001550300	BCIN_05g00350 (<i>bcnoxA</i>)	1.57	NADPH oxidase (NOX)	Pathogenicity, fusion of conidial anastomosis tubes, and formation of sclerotia and conidia
cro-mir-4	XM_024690414	BCIN_01g03790 (<i>bccshIV</i>)	1.54	Chitin synthase	Cell wall biosynthesis, development and pathogenicity
cro-mir-4	XM_024692792	BCIN_05g00540 (<i>bchhkr1</i>)	1.47	Protein kinase	Signal transduction b
cro-mir-13 and cro-mir-2	XM_001551683	BCIN_09g06130 (<i>bcpls1</i>)	1.4	Tetraspanins	Appressorium development, host penetration
cro-mir-1 and cro-mir-2	XM_001547152	BCIN_12g05700	1.38	Cyclases	Biosynthesis of lantibiotics
cro-mir-36	XM_001554608	BCIN_08g03180	1.26	Transcription factor	Appressorium formation
cro-mir-36	XM_024694081	BCIN_07g04590 (<i>bchsts1</i>)	1.2	Histidine-tRNA ligase	Translation, ribosomal structure, and biogenesis
cro-mir-4 and cro-mir-36	XM_024695521	BCIN_10g02810 (<i>bcyta7</i>)	1.13	Bromodomain-containing protein	Chromatin remodeling
cro-mir-1 and cro-mir-2	XM_024694912	BCIN_09g01210 (<i>bccsh1</i>)	1.11	Chitin synthase	Cell wall biosynthesis, virulence
cro-mir-13	XM_024697868	BCIN_16g01130 (<i>bcpkar1</i>)	1.03	Serine/threonine kinases	Conidial germination, growth, and virulence
cro-mir-5	XM_024694566	BCIN_08g03270 (<i>bcvac8</i>)	1.02	Fungus-type vacuole membrane	Intracellular trafficking and secretion
<i>Fusarium graminearum</i>					
cro-mir-3	XM_011328464	FGSG_07067	1.41	Transcription factor	Virulence
cro-mir-4	XM_011319656	FGSG_02083	1.02	Transcription factor	Mycotoxin biosynthesis
cro-mir-5	XM_011317736	FGSG_00376	1.07	Ubiquinone oxidoreductase	Virulence
cro-mir-5	XM_011321023	FGSG_13747	1.03	Membrane transporter	Transmembrane transporter activity
cro-mir-5	XM_011329154	FGSG_07665	1.14	Membrane transporter	Transmembrane transporter activity
cro-mir-1 and cro-mir-2	XM_011319110	FGSG_11973	1.44	Membrane transporter	Transmembrane transporter activity
cro-mir-9	XM_011329717	FGSG_09686	1.58	Vesicle-mediated transport	Intracellular trafficking and secretion
cro-mir-6	XM_011326744	FGSG_06384	1.11	Vesicle-mediated transport	Intracellular trafficking and secretion

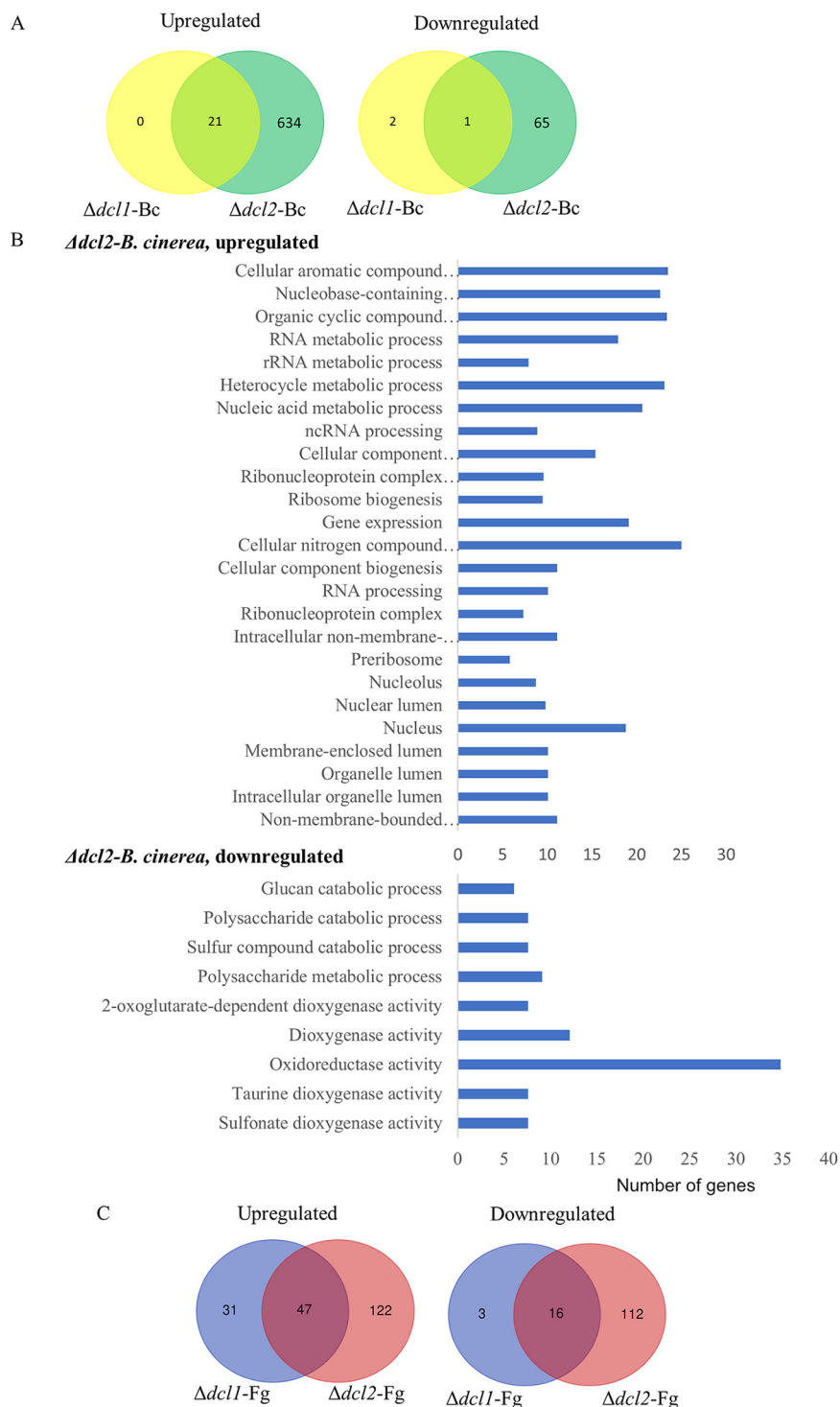


FIG 6 Transcriptome analysis of *B. cinerea* (Bc) and *F. graminearum* (Fg) during the interaction with *dcl1* and *dcl2* deletion strains compared to those of the WT. (A) Venn diagrams showing the overlap between upregulated and downregulated genes in the $\Delta dcl1$ and $\Delta dcl2$ strains during the interactions with *B. cinerea* compared to the WT. (B) Gene Ontology terms enriched in upregulated and downregulated genes in *dcl2* deletion strains during the interactions with *B. cinerea*. (C) Venn diagrams showing the overlap between up- and downregulated genes in $\Delta dcl1$ and $\Delta dcl2$ strains during interactions with *F. graminearum* compared to the WT.

TABLE 6 Differential expression patterns of selected genes in *B. cinerea* and *F. graminearum* during interaction with $\Delta dcl1$ and $\Delta dcl2$ mutants compared to those of wild-type *C. rosea* and the same mycohost

GenBank accession no.	Locus tag (gene ID)	Gene function	Expression (log ₂ FC) ^a		Biological function
			$\Delta dcl1$	$\Delta dcl2$	
<i>Botrytis cinerea</i>					
XM_001547559	BCIN_02g08360 (bcfrq1)	Circadian oscillator	1.05	2.03	Virulence
XM_001550300	BCIN_05g00350 (bcnoxa)	NADPH oxidase complex	-0.39	1.57	Virulence
XM_001552181	BCIN_12g03770 (bcnop53)	Pre-rRNA processing factor	0.19	1.59	Fungal development and pathogenesis
XM_001555445	BCIN_03g06840 (bcnoxr)	Regulatory subunit of NOX (NADPH oxidase regulator)	-0.01	1.56	Differentiation and pathogenicity
XM_024691832	BCIN_03g02630 (bcste11)	MAPK triple kinase	0.16	1.81	Hypal growth
XM_024693262	BCIN_06g00026 (mfsG)	Major facilitator superfamily transporter	-0.84	-5.95	Tolerance to glucosinolate-breakdown products, required for pathogenicity
XM_024697209	BCIN_14g03930 (bc1tf1)	GATA transcription factor	1.66	3.86	Tolerance to oxidative stress, virulence
XM_024697551	BCIN_15g03390 (bcvel1)	Regulatory protein of the VELVET complex	0.13	1.59	Formation of oxalic acid, virulence
XM_024694938	BCIN_09g01620 (bccry2)	DNA photolyase	1.74	3.57	Negative regulation of filamentous growth and conidiation
XM_001561274	BCIN_01g06010 (bccrh)	Transglycosylase	0.00	1.83	Cell wall biogenesis, virulence
XM_024693846	BCIN_07g01300 (bccshvii)	Chitin synthase	0.06	1.83	Cell wall biogenesis, virulence
XM_024696504	BCIN_12g05360 (bccshvi)	Chitin synthase	0.04	1.66	Cell wall biogenesis, Virulence
XM_001545464	BCIN_12g05370 (bccshv)	Chitin synthase	-0.12	1.63	Cell wall biosynthesis
XM_024690414	BCIN_01g03790 (bccshiv)	Chitin synthase	-0.15	1.54	Cell wall biosynthesis
XM_001554790	BCIN_03g09000	Septin GTPase	2.87	5.60	Cytoskeleton-dependent cytokinesis (septin ring)
XM_024693922	BCIN_07g02420	MFS transporters	-0.83	2.99	Xenobiotic transport
XM_024695797	BCIN_11g00800	Protein kinase CK2	1.43	2.96	Regulates various cellular processes
XM_024690261	BCIN_01g01760	Chitinase activity	0.06	2.67	Cell wall biosynthesis
XM_024696411	BCIN_12g03920	Chitin binding	0.35	2.22	Chitin recognition
XM_001549884	BCIN_01g02970	Chitin binding	0.00	1.96	Chitin recognition
XM_024693364	BCIN_06g01930 (bcgo1)	Chitin binding	-0.07	1.87	Chitin recognition
XM_001547426	BCIN_01g00360 (bcerg1)	Squalene monoxygenase	1.55	2.74	Sterol biosynthetic process
<i>Fusarium graminearum</i>					
XM_011317671	FGSG_00324 (<i>fgmyt3</i>)	Transcription factor	+1.05	+1.52	Fungal development and pathogenicity
XM_011318135	FGSG_00729 (<i>gzlmg005</i>)	Transcription factor	+0.99	+1.56	Virulence
XM_011320684	FGSG_10057 (<i>fgerb1</i>)	Transcription factor	+1.44	+1.52	Growth and pathogenicity
XM_011321826	FGSG_08617 (<i>gzczh066</i>)	Transcription factor	+1.46	+1.84	Virulence
XM_011322702	FGSG_04580 (<i>fgabc1</i>)	ABC pleiotropic drug resistance transporter	+1.72	0.40	Virulence and tolerance to benalaxyl
XM_011327033	FGSG_11028	Multidrug resistance-associated protein		+2.65	Valenol biosynthesis
XM_011326203	FGSG_05898 (<i>fgplc1</i>)	Fungal phospholipase C	+1.31	+1.66	Development, pathogenicity, and stress responses
XM_011328541	FGSG_07133 (<i>gzczc30</i>)	Transcription factor	+1.18	+1.72	Virulence
XM_011329465	FGSG_07928 (<i>gzczh059</i>)	Transcription factor	+1.29	+1.61	Virulence
XM_011317284	FGSG_00007	Cytochrome P450	-3.85	-3.68	DON biosynthesis
XM_011317365	FGSG_00071 (<i>tri1</i>)	Cytochrome P450	-1.62	-1.38	DON biosynthesis
XM_011323873	FGSG_03534 (<i>tri3</i>)	15-O-Acetyltransferase	-2.99	-4.17	DON biosynthesis

(Continued on next page)

TABLE 6 (Continued)

GenBank accession no.	Locus tag (gene ID)	Gene function	Expression (log ₂ FC) ^a		Biological function
			$\Delta dcl1$	$\Delta dcl2$	
XM_011323872	FGSG_03535 (<i>tri4</i>)	Trichodiene oxygenase	-3.24	-5.12	DON biosynthesis
XM_011323870	FGSG_03537 (<i>tri5</i>)	Trichodiene synthase	-2.74	-3.56	DON biosynthesis
XM_011323871	FGSG_03536 (<i>tri6</i>)	Transcription factor	-1.15	-1.65	DON biosynthesis
XM_011323868	FGSG_03539 (<i>tri9</i>)	TRI9 protein	-1.42	-1.84	DON biosynthesis
XM_011323864	FGSG_03543 (<i>tri14</i>)	Mala s 1-allergenic	-2.67	-3.91	DON biosynthesis
XM_011323865	FGSG_03542	Cytochrome P450	-1.81	-5.13	DON biosynthesis
XM_011322312	FGSG_08196	Peptidase A4	-3.30	-5.00	Highly induced in mycotoxin-inducing media
XM_011324413	FGSG_03065 (<i>gzcarb</i>)	Phytoene dehydrogenase	-0.80	-2.08	Neurosporaxanthin and torulene BGC
XM_011324406	FGSG_03071	FAD-dependent oxidoreductase	-1.74	-3.26	Neurosporaxanthin and torulene BGC
XM_011324412	FGSG_03066 (<i>gzcarra</i>)	al-2/carRA phytoene synthase	-0.77	-1.58	Neurosporaxanthin and torulene BGC
XM_011321137	FGSG_10460 (<i>fs15</i>)	Enoyl reductase	1.10	-4.27	Fusarielin BGC
XM_011321139	FGSG_10462 (<i>fs3</i>)	Aldose 1-epimerase	1.54	-2.45	Fusarielin BGC
XM_011321140	FGSG_10463 (<i>fs2</i>)	Esterase	1.78	-2.03	Fusarielin BGC
XM_011321141	FGSG_10464 (<i>fs1</i>)	Polyketide synthase	1.52	-1.87	Fusarielin BGC

^aSignificant differences (FDR < 0.05 and log₂FC > 1.5 or < -1.5) are highlighted in boldface letters.

activity (GO:0016491), oxidation-reduction processes (GO:0055114), and polysaccharide and glucan catabolic processes (GO:0000272 and GO:0009251) were enriched for the downregulated genes (Fig. 6B).

During $\Delta dcl2$ mutant-*F. graminearum* interaction, 397 (169 upregulated and 128 downregulated) *F. graminearum* genes were differentially expressed, while only 97 (78 upregulated and 19 downregulated) were differentially expressed during the $\Delta dcl1$ -*F. graminearum* interaction (Fig. 6C; see also Table S6D). Totals of 47 and 16 genes were upregulated and downregulated, respectively, against both mutant strains, whereas the rest were differentially expressed only during contact with one of the mutants (Fig. 6C). Furthermore, we found 26 (9 upregulated and 17 downregulated) previously characterized *F. graminearum* genes that were differentially regulated during the interaction with *dcl* deletion strains compared to the WT (Table 6). The downregulated genes included several involved in deoxynivalenone, neurosporaxanthin, torulene, and fusarielin biosynthesis. Moreover, eight of the nine upregulated genes were previously characterized for having a role in *F. graminearum* virulence, and six of them encoded transcription factors (FgMYT3, GzHMG005, FgERB1, GzC2H066, GzZC230, and GzC2H059) (Table 6). Additionally, during the interaction with the $\Delta dcl2$ mutant, 14 *F. graminearum* CAZyme genes showed upregulation with respect to the WT, all of them predicted to encode glycoside hydrolases, whereas only 3 genes were downregulated. MFS transporters were among the DEGs as well, with five of them being upregulated while seven were downregulated (see Table S6D).

DISCUSSION

While the $\Delta dcl1$ mutant had a phenotype largely similar to the WT, the $\Delta dcl2$ mutant displayed evident differences, including a higher number of differentially expressed genes during the interaction with the plant-pathogenic mycohosts. This number of DEGs was significantly higher than the number of genes predicted to be directly targeted from DCL2-regulated miRNAs, but it has already been observed in *F. graminearum* and *T. atroviride* how RNAi can be involved in regulating the activity of transcription factors and other regulatory elements and therefore indirectly influencing the expression of a vast array of genes and pathways (20, 69). In our data set, we could observe four *C. rosea* transcription factors downregulated in the WT during interaction with the mycohosts and putatively targeted by miRNAs downregulated in the $\Delta dcl2$ mutants. Among these, CRV2G00015277 and CRV2G00002266 were involved in the interaction with both the mycohosts, while CRV2G00002043 was involved only in response to *B. cinerea*. CRV2G00002266 exhibited significant sequence similarities with the PRZ1 transcription factor, known for regulating the expression of the vacuolar ATPase Ca^{2+} pump PMC1 (71). This pump shown to regulates the level of cytoplasmic Ca^{2+} by activating Ca^{2+} -dependent enzymes involved in protein secretion in the nuclear envelope, endoplasmic reticulum, Golgi complex, and *trans*-Golgi/endosomal network in *S. cerevisiae* (71).

Furthermore, several other putative miRNA targets could have regulatory roles, including the predicted helicases CRV2G00001868 and CRV2G00004339 and the putative Rho-type GTPase activating protein CRV2G00008014. In particular, the transcript of gene CRV2G00004339, putatively targeted by miRNAs during interaction with *F. graminearum*, encodes a helicase of superfamily SNF2, involved in chromatin remodeling by deposition of H2A (72).

Beyond the direct action of miRNAs on targets, the deletion of *dcl1* and especially *dcl2* induced the differential expression of several secondary metabolite BGCs in *C. rosea*. The BGC containing the PKS gene *pks22*, involved in the synthesis of the antifungal compound clonorosein (50) was downregulated in the $\Delta dcl2$ mutant during the interaction with both mycohosts. In contrast, no difference in clonorosein A production was detected between the WT and the *dcl* mutants in the metabolome analysis. However, since the metabolome analysis was performed under *in vitro* conditions, it is possible that the *dcl2*-dependent regulation of clonorosein production is more pronounced during contact with the mycohosts. In fact, *pks22* was previously shown to be induced during interactions with *B. cinerea* and *F. graminearum* (50). The sorbicillin BGC, responsible for the yellow coloration

of WT *C. rosea* colonies (50), is downregulated in the $\Delta dcl2$ mutant, and both sorbicillin and sorbicillinol were underproduced in the $\Delta dcl2$ mutant and had their biosynthesis restored in the complementation mutant in the *in vitro* trials, explaining the difference in pigmentation of the $\Delta dcl2$ mutant. This gene cluster was also induced during the interaction of *C. rosea* strain ACM941 with *F. graminearum* in the study of Demissie et al. (48). However, it is interesting that the positive regulator of the cluster, YPR1 (CRV2G00015416), is not differentially expressed in our study, whereas the transcription factor YPR2 (CRV2G00015419) is downregulated and hence coregulated with the other genes in the gene cluster in the $\Delta dcl2$ mutant. YPR2 is a Gal4-like transcription factor predicted to positively regulate a negative regulator of sorbicillin biosynthesis (62), and its coregulation with the biosynthetic genes suggests that the deletion of DCL2 affects the control of sorbicillin production at a currently unknown level.

Furthermore, two putatively important BGCs were specifically downregulated in the $\Delta dcl2$ mutant during contact with *F. graminearum*: these were the *pks29* BGC involved in antagonism and biocontrol (50) and the BGC with the NRPS-like CRV2G00015275 as the core enzyme. This last cluster was studied as “cluster 3” in the work of Demissie et al. (47), where it was found to be induced in *C. rosea* after exposure to the *F. graminearum* secretome, and it presents strong homology with the fumisoquin cluster of *Aspergillus fumigatus* (73). Deletion of the core NRPS-like enzyme of the cluster leads to reduced growth and sporulation in *A. fumigatus* (74), but fumisoquins were not produced in detectable amounts by either the WT or the $\Delta dcl2$ mutant in our *in vitro* analysis. Biosynthesis of the corresponding compound in *C. rosea* may be specifically triggered during contact with *F. graminearum*. The transcription factor CRV2G00015277, putatively targeted by DCL2-dependent novel miRNAs cro-mir-5, cro-mir-10, and cro-mir-11, is located next to the cluster and is upregulated in the $\Delta dcl2$ mutant. It is possible that CRV2G00015277 is a negative regulator of the cluster, targeted by miRNAs to induce the production of fumisoquins, but this hypothesis should be examined in a future study. None of these gene clusters (sorbicillin, clonoroseins, *pks29*, and fumisoquins) were downregulated in the $\Delta dcl1$ mutant. The reduced production of bisorbicillinol in the $\Delta dcl2$ mutant also suggests that the deletion might hamper this fungus' antibacterial properties, since several bisorbicillinoids synthesized by *C. rosea* have significant antibacterial activity (75).

A further reason for the diminished capacity of the $\Delta dcl2$ mutant to control the plant-pathogenic mycohosts can be found in the downregulation of genes encoding enzymes involved in the degradation of the fungal cell wall. In the $\Delta dcl2$ mutant, between 55 and 64 glycoside hydrolase genes were downregulated compared to the WT. Among these were three GH18 chitinases (*ech37*, *ech42*, and *chiA5*) and one GH20 *N*-acetylhexosaminidase (CRV2G00012950), which were downregulated during interaction with both mycohosts. Furthermore, four genes putatively involved in cell wall degradation of *F. graminearum* (48) were found to be downregulated in the $\Delta dcl2$ mutant: these were two glycoside hydrolases of classes GH2 (CRV2G00016896) and GH114 (CRV2G00003509), as well as two metallopeptidases (CRV2G00010851 and CRV2G00011092). Interestingly, the gene *chiC1*, predicted to encode a killer toxin-like chitinase that permeabilizes the cell wall of antagonistic species to facilitate entry of toxic metabolites (76, 77), is upregulated in the $\Delta dcl2$ mutant. This may be explained by the fact that *chiC1* is induced by chitin (44) and that the $\Delta dcl2$ mutant is compromised in its ability to antagonize the mycohosts, resulting in larger amounts of chitin exposed to the $\Delta dcl2$ mutant.

Moreover, 17 genes upregulated during *C. rosea* response to mycohosts in the study of Nygren et al. (49) were downregulated in the $\Delta dcl2$ mutants in comparison with the WT upon contact with the same mycohost. Among them is a putative isotrichodermin C-15 hydroxylase (*cyp1*), a type of protein also induced during mycoparasitism in *T. cf. harzia-num* (78), but the majority of these genes is constituted by transporters, especially MFS transporters. This group includes gene *mfs464*, suggested in the study of Nygren et al. (49) to perform an important function in the mycoparasitic attack against *F. graminearum*, due to its extreme induction (fold change > 693). *mfs166* and *mfs464*, downregulated in the

Δdcl2 mutant, were found to be upregulated during the *C. rosea* response to *F. graminearum* in the studies of both Nygren et al. (49) and Demissie et al. (48), making their involvement in response to the mycohost very likely. The other detected differentially expressed MFS transporters are commonly involved in efflux-mediated protection against exogenous or endogenous secondary metabolites and sugar uptake, suggesting a DCL-dependent influence on this aspect of *C. rosea* mycoparasitic action. This group also includes nine genes belonging to the drug-H⁺ antiporter-2 family, which underwent a significant gene expansion during *C. rosea* evolution and has therefore a putative important role in the fungus lifestyle (79). DCL-based control of these transporters is most likely indirect because most MFS genes detected in this way are downregulated in the mutants, whereas direct targets of RNA silencing are expected to be upregulated after *dcl* deletion. Reinforcing this hypothesis, none of the MFS transporters predicted in *C. rosea* is a putative target of differentially expressed miRNAs detected in this study. Identification of several upregulated genes coding for MFS transporters used by mycohosts to tolerate harmful secondary metabolites of their own production strengthens the hypothesis that these proteins enable *C. rosea* to withstand mycohost-produced toxins during fungus-fungus interaction.

The differential expression of this vast number of genes is likely due to the 128 putative transcription factors differentially expressed in the *Δdcl2* mutant. Among these, CRV2G00006707 is a homolog of the CCAAT-binding subunit HAP3, regulating growth and secondary metabolism in other filamentous fungi such as *F. verticillioides* (68, 80). This gene is downregulated in the *Δdcl2* mutant during interaction with both mycohosts (log₂ fold change [log₂FC] of -1.6 in Cr-Bc [*C. rosea* + *B. cinerea*] and -1.3 in Cr-Fg [*C. rosea* + *F. graminearum*]). Another transcription factor downregulated in the *Δdcl2* mutant was CRV2G00004759, a homolog of the filamentous growth regulator 27 (*fgf27*) of *Trichoderma lentiforme*, which is involved in adherence regulation and could have a role in reduced growth rate of the mutant (67). Moreover, two putative homologs of the sucrose utilization protein 1 (SUC1) are upregulated in the *Δdcl2* mutant, and its upregulation is associated with a delay in mitotic and meiotic nuclear divisions in *Schizosaccharomyces pombe* (66).

It is possible that part of the reduced ability of the *Δdcl2* mutant to overgrow *B. cinerea* *in vitro* and control *F. graminearum* *in vivo* comes from a cross-regulating action of *C. rosea* miRNAs targeting mycohost genes involved in the development or reduction of virulence. Specifically, three *F. graminearum* virulence factors were both downregulated during interaction with the WT *C. rosea* and putatively targeted by miRNAs downregulated in the *Δdcl2* mutants. These genes included FGSG_07067, the GzZC232 transcription factor whose deletion impaired virulence in the work of Son et al. (81); FGSG_00376, the NOS1 NADH ubiquinone oxidoreductase proven to be a factor of virulence by Seong et al. (82); and FGSG_02083, the transcription factor ART1, whose deletion causes reduced starch hydrolysis and virulence, as well as the incapability of trichothecenes biosynthesis (83). Regarding *B. cinerea*, among the putative miRNA-targeted downregulated genes, there were those encoding BCIN_09g06130, the BcPIs1 tetraspanin necessary for appressorium-mediated penetration into host plant leaves (84), and BCIN_16g01130, the *bcpka1* catalytic subunit of the cAMP-dependent protein kinase, whose deletion affects the lesion development and leaves rot caused by the fungus (85). Two other putative targets were BcnoxA (BCIN_05g00350), a component of the *B. cinerea* NADPH oxidase complex necessary for the colonization of host tissues (86), and the MAP triple kinase BcSte11 (BCIN_03g02630), whose deletion is known to cause defects in germination, delayed vegetative growth, reduced size of conidia, lack of sclerotium formation, and loss of pathogenicity in *B. cinerea* (87). Moreover, a *B. cinerea* homolog of *Ssams2* (BCIN_08g03180) was also among the putative targets, and this gene encodes a GATA transcription factor required for appressoria formation and chromosome segregation in *S. sclerotiorum* (70).

Several other genes encoding virulence factors were found to be upregulated in the pathogenic mycohosts during the interaction with the *Δdcl2* mutant, even if they were not among the putative targets of miRNAs. Among the *F. graminearum* genes upregulated during contact with the *Δdcl2* mutant were the transcription factors MYT3, ERB1,

GzHMG005, GzC2H066, GzZC230, and GzC2H059, whose disruption reduces the virulence of the pathogen (81, 88–91), as well as the phospholipase PLC1, known for its involvement in hyphal growth, conidiation, deoxynivalenol production, and virulence (92). Regarding *B. cinerea*, among the genes upregulated during contact with the $\Delta dcl2$ mutant, we found *nop53* and *noxR*, crucial for fungal development and virulence through the regulation of reactive oxygen species (93, 94); *frq1*, involved in circadian regulation of fungal virulence (95); and *vel1*, whose deletion affects virulence and light-dependent differentiation (96). Moreover, among the upregulated genes there was also a homolog (BCIN_14g03930) of the *S. sclerotiorum* transcription factor *SsNsd1*, necessary for pathogenicity and appressorium formation (97). Furthermore, upon contact with the $\Delta dcl2$ mutant, *B. cinerea* upregulated several genes encoding proteins involved in chitin and cell wall synthesis, such as *Bccrh1*, *BcchsIV*, *BcchsV*, *BcchsVI*, and *BcchsVII* (98–101). The upregulation of *BcCHSVI* and *BcCHSVII* is of particular interest because these proteins have a role in plant infection (101).

Genes encoding two virulence factors of *F. graminearum* (TRI5 and TRI6) and one of *B. cinerea* (MFSG) were downregulated during interaction with the $\Delta dcl2$ mutant. The gene *mfsG* is involved in *B. cinerea* virulence by providing tolerance to glucosinolate-breakdown products (102), but the *C. rosea* $\Delta dcl2$ mutant shows downregulation in several putative secondary metabolite clusters compared to the WT. Therefore, it is possible that the expression of *mfsG* is reduced during contact with the mutant because the lack of production of harmful compounds makes it unnecessary for the mycohost to express resistance genes. TRI5 and TRI6 are involved in the synthesis of trichothecenes (103, 104), and other genes involved in the biosynthesis of these mycotoxins are similarly downregulated during contact with the $\Delta dcl2$ mutant, including the genes *TRI1*, *TRI3*, *TRI4*, *TRI9*, and *TRI14* (105). This is surprising because *F. graminearum* overexpresses the transcription factor gene *ART1* during contact with the $\Delta dcl2$ mutant, and this transcription factor is known to be a positive regulator of trichothecene biosynthesis (83). The reduced ability of the $\Delta dcl2$ mutant to control *F. graminearum* may make it unnecessary for the mycohost to produce DON in high quantities, despite *ART1* overexpression. Interestingly, among the most relevant genes proven to be DON-responsive in *C. rosea* in a previous study (106), only 1 of 16 was found to be less expressed in the $\Delta dcl2$ mutant than in the WT during interaction with *F. graminearum*: a homolog of glucose repressible protein GRG1 (CRV2G00000966). Given the reduced expression of DON-biosynthesis genes by *F. graminearum*, the downregulation of a higher number of DON-responsive genes was expected.

Another important mycotoxin produced by *F. graminearum* is zearalenone, and the zearalenone hydrolase gene *zhd101* (CRV2G00011056) was found to be downregulated by the $\Delta dcl2$ mutant. The deletion of this gene undermines *C. rosea* mycoparasitic action against *F. graminearum* (107), and its downregulation is therefore a possible reason for the impaired biocontrol action of the $\Delta dcl2$ mutant. Another zearalenone-responsive gene, one encoding a putative bacteriorhodopsin-like protein (106), is also downregulated in the $\Delta dcl2$ mutant, but its role in the *C. rosea*-*F. graminearum* interaction is still unknown.

Interestingly, *F. graminearum* showed altered production of red pigment at the point of contact with the $\Delta dcl2$ mutant, which could plausibly be due to downregulation of genes belonging to the gene clusters of carotenoid and fusarielin (108, 109). However, the gene cluster of aurofusarins, known for their red colorations, was not differentially expressed during the interaction with the $\Delta dcl2$ mutant.

Conclusions. DCL-dependent RNA silencing plays a determinant role in the regulation of many biological processes. In the present study, the role of DCL-like enzymes was investigated for the first time in the antagonistic action of the fungus *C. rosea*. Our results show that DCL2-mediated RNAi plays a central role in regulating endogenous cellular processes involved in growth, secondary metabolite production, and antagonism toward the mycohosts, whereas the function of DCL1 is redundant except for conidium production. The observed phenotypic effect in $\Delta dcl2$ strains is due to the diminished production of antifungal metabolites in the mutant, as well as to downregulation of genes known

to be involved in mycohost response and resistance to secondary metabolites. Identification of 11 miRNAs, which were downregulated in the $\Delta dcl2$ strain, and their putative endogenous gene targets, including transcription factors and chromatin remodeling proteins, indicates DCL-dependent regulation of *C. rosea* antagonistic interactions. Furthermore, we predicted putative cross-species gene targets in the mycohosts *B. cinerea* and *F. graminearum* previously characterized for their role in fungal virulence, posing the bases for future studies focusing on the role of DCL-dependent RNA silencing in interspecific fungal interactions.

MATERIALS AND METHODS

Fungal strains and culture conditions. *C. rosea* strain IK726 WT and mutants derived from it, *B. cinerea* strain B05.10, and *F. graminearum* strain PH1 were used in this study. The fungal cultures were maintained on PDA (Oxoid, Cambridge, UK) medium at 25°C.

Gene identification and phylogenetic analysis. *C. rosea* strain IK726 genome version 1 (41) and version 2 (55) were screened for the presence of genes encoding DCL, AGO, and RDR by BLASTP analysis. The presence of conserved domains was analyzed using the Simple Modular Architecture Research Tool (SMART) (110), InterProScan (111), and conserved domain search (112).

Amino acid sequences of DCLs (DCL1 and DCL2), AGOs (AGO1 and AGO2), and RDRPs of several fungal species (see Table S1A) were retrieved from the UniProt and GenBank databases (113, 114). The sequences of Dicer1, Argonaute1, and RDR of the model plant *Arabidopsis thaliana* were retrieved from the UniProt database (113) and used as outgroups. Sequences were aligned with mafft v.7 (115) with options suggested for <200 sequences (L-INS-i), and the phylogenetic trees were generated using iqtree v.1.6.12 (116) with 1,000 bootstrap replicates and option "MFP" to find the best substitution model. Figtree v.1.4.4 (117) was used to visualize the trees.

Construction of deletion vector, transformation, and mutant validation. The ~1-kb 5'-flank and 3'-flank regions of *dcl1* and *dcl2* were amplified from genomic DNA of *C. rosea* using gene-specific primer pairs (see Table S1B), as indicated in Fig. S1 (53). Gateway cloning system (Invitrogen, Carlsbad, CA) was used to generate entry clones of the purified 5'-flank and 3'-flank PCR fragments as described by the manufacturer (Invitrogen, Carlsbad, CA). The hygromycin resistance cassette (*hygB*) generated during our previous studies (43, 118) from pCT74 vector, as well as a Geneticin resistance cassette generated as a PCR product from the pUG6 vector (119), were used. A three-fragment multisite gateway LR recombination reaction was performed using the entry plasmids of respective fragments and destination vector pPm43GW (120) to generate the deletion vectors. Complementation cassettes for *dcl1* and *dcl2* were constructed by PCR amplification of the full-length sequence of *dcl1* and *dcl2*, including ~800-bp upstream and ~500-bp downstream regions from genomic DNA of *C. rosea* WT using gene-specific primers (see Table S1B). The amplified DNA fragments were purified and integrated into destination vector pPm43GW using two-fragment gateway cloning technology to generate complementation vectors.

Agrobacterium tumefaciens-mediated transformation was performed based on a previous protocol for *C. rosea* (43, 121). Transformed strains were selected on plates containing either hygromycin for gene deletion or Geneticin for complementation. Validation of homologous integration of the deletion cassettes in putative transformants were performed using a PCR screening approach with primer combinations targeting the *hygB* cassette and sequences flanking the deletion cassettes (see Fig. S1), as described previously (45, 122). PCR-positive transformants were tested for mitotic stability and then purified by two rounds of single-spore isolation (118). To determine the transcription of *dcl1* and *dcl2* in the WT, deletion, and complementation strains, total RNA from the respective strains were isolated (Qiagen, Hilden, Germany). After DNase I treatment, according to the manufacturer's instructions (Merck, Kenilworth, NJ) reverse transcription-PCR (RT-PCR) was performed using RevertAid premium reverse transcriptase (Fermentas, St. Leon-Rot, Germany) and gene-specific primer pairs (see Table S1B).

Phenotypic analyses. Phenotypic analyses experiments were performed with *C. rosea* WT, deletion strains *dcl1* ($\Delta dcl1$) and *dcl2* ($\Delta dcl2$), and their respective $\Delta dcl1+$ and $\Delta dcl2+$ complemented strains. Each experiment was repeated twice with similar results.

The growth rate, colony morphology, and conidium production were analyzed in four biological replicates as described previously (43). To analyze mycelial biomass, agar plugs of *C. rosea* strains were inoculated in 50-ml conical flasks with 20 ml of PDB (Oxoid, Cambridge, UK), followed by incubation at 25°C under constant shaking (100 rpm). Biomass production was determined by measuring the mycelial dry weight 5 days postinoculation. The antagonistic behavior against *B. cinerea* and *F. graminearum* was tested using an *in vitro* plate confrontation assay on PDA medium, as described previously (51). The growth of *B. cinerea* and *F. graminearum* was measured daily until their mycelial fronts touched the *C. rosea* mycelial front. The experiments were performed in four biological replicates. The biocontrol ability of *C. rosea* strains against *F. graminearum* was evaluated in a *fusarium* foot rot assay, as described previously (123). In brief, surface sterilized wheat seeds were treated with *C. rosea* conidia (1×10^7 conidia/ml) in sterile water, sown in moistened sand, and kept in a growth chamber after pathogen inoculation (51). Plants were harvested 3 weeks postinoculation, and disease symptoms were scored on scale of 0 to 4, as described previously (51, 123). The experiment was performed in five biological replicates with 15 plants in each replicate.

Statistical analysis. ANOVA was performed on phenotype data using the general linear model approach implemented in Statistica version 16 (TIBCO Software, Inc., Palo Alto, CA). Pairwise comparisons were made using the Tukey-Kramer method at a 95% significance level.

Metabolite analysis. An agar plug of *C. rosea* strains was inoculated on PDA (Oxoid) and allowed to grow for 10 days at 25°C. Agar plugs, together with mycelia, were harvested from the centers of plates using 50-ml Falcon tubes (53). The mycelial plug was sonicated for 15 min in 20 ml of methanol, and then 1 ml of extract was transferred to a 1.5-ml centrifuge tube for centrifugation at $10,000 \times g$ for 5 min. Supernatants were collected and then analyzed by UHPLC-MS on a reversed-phase column (2.1 \times 50 mm, 1.5 μ m; Accucore Vanquish; Thermo Scientific, Waltham, MA) using a gradient of acetonitrile (MeCN) in water, both with 0.2% formic acid (10 to 95% MeCN in 3 min and 95% MeCN for 1.2 min, at 0.9 ml min⁻¹). The MS was operated in positive mode with scanning of m/z 50 to 1,500, and the mass spectra were calibrated against sodium formate clusters using the Compass DataAnalysis 4.3 software (Bruker Daltonics, Bremen, Germany) that was also used for general data analysis. UHPLC-MS/MS was run with the same instrument, column, and UHPLC conditions, using the auto-MS/MS function (1+ precursor ions, m/z 50 to 1,500, with ramped fragmentation energies of 20/30/35 eV for m/z 200/500/1,000). The UHPLC-MS data were converted to mzXML format using DataAnalysis 4.3, and ion chromatogram peak picking in the range 5 to 200 s was performed using the program XCMS in software environment R using the centWave method (peak width, 3 to 20 s; m/z tolerance, 5 ppm; noise, 1,000) (124, 125). XCMS was used for subsequent peak grouping and missing peak filling. For each sample, the resulting molecular feature peak areas were normalized against the sum of peak areas, and the resulting relative peak areas were 10 logarithmized. The data were used for PCA, and ANOVA was used to evaluate significant differences in concentrations between strains. Tentative compound identification was done by comparing high-resolution mass spectrometry data on fungal compounds from the databases Antibase and combined chemical dictionary. The identity of the tentatively identified compounds was further corroborated by analysis of MS/MS data. The experiment was performed in five biological replicates.

Dual culture interaction experiment for sRNA and transcriptome sequencing. An agar plug of *C. rosea* strains was inoculated at edge of a 9-cm-diameter PDA (Merck, Kenilworth, NJ) petri plate covered with a Durapore membrane filter (Merck) for easy harvest of mycelia. The mycohost fungi *B. cinerea* or *F. graminearum* were inoculated at opposite side of the plate (43). Due to different mycelial growth rates, *C. rosea* was inoculated 7 days prior to the inoculation of *F. graminearum* or *B. cinerea*. The mycelial front (5 mm) of *C. rosea* was harvested together with the mycelial front (5 mm) of *B. cinerea* (Cr-Bc) or *F. graminearum* (Cr-Fg) at the hyphal contact stage of interactions (see Fig. S2A) and snap-frozen in liquid nitrogen. The experiment was performed in three biological replicates.

RNA extraction, library preparation, and sequencing. Total RNA was extracted using the mirVana miRNA isolation kit according to the manufacturer's protocol (Invitrogen, Waltham, MA). The RNA quality was analyzed using a 2100 Bioanalyzer Instrument (Agilent Technologies, Santa Clara, CA) and concentration was measured using a Qubit fluorometer (Life Technologies, Carlsbad, CA). For sRNA and mRNA sequencing, the total RNA was sent for library preparation and paired-end sequencing at the National Genomics Infrastructure (NGI), Stockholm, Sweden. The sRNA library was generated using TruSeq small RNA kit (Illumina, San Diego, CA), while the mRNA library was generated using a TruSeq Stranded mRNA Poly(A) selection kit (Illumina, San Diego, CA). The sRNA and mRNA libraries were sequenced on a NovaSeq SP flow cell with a 2 \times 50-bp reads and NovaSeqXp workflow in S4 mode flow cell with 2 \times 151 setup, respectively, using Illumina NovaSeq6000 equipment at NGI Stockholm. The Bcl to FastQ conversion was performed using bcl2fastq_v2.19.1.403 from the CASAVA software suite (126). The quality scale used was Sanger/phred33/Illumina 1.8+.

(i) Functional annotation of genomes. The predicted proteomes of *C. rosea* strain IK726, *B. cinerea* strain B05.10 (ASM14353v4), and *F. graminearum* strain PH-1 (ASM24013v3) were annotated through BLAST2GO v.5.2.5 (127) and InterProScan v.5.46-81.0 (111) with default parameters to identify transcription factors. Secondary metabolite clusters were predicted through antiSMASH v.5.0 (128), while predicted enzymes involved in the metabolism of carbohydrates (CAZymes) were identified using the dbCAN2 meta-server (129). The amino acid sequences of *B. cinerea* and *F. graminearum* were compared to the PHI-base database using BLAST (130) with a minimum of 80% in both identity and query coverage. All identified matches described in the PHI-base annotation by the keywords "reduced virulence" or "loss of pathogenicity" were considered to be potential virulence factors.

(ii) Differential expression and GO enrichment analyses. Reads were trimmed with bbduk v.38.86 (131) with the following options: bbduk.sh in1=read1.fastq in2=read2.fastq out1=read1_clean.fastq out2=read2_clean.fastq ref=reference.fa ktrim=r k=23 mink=11 hdist=1 tpe tbo qtrim=r trimq=10. Successful cleaning and adapter removal was verified with fastqc v. 0.11.9 (<https://www.bioinformatics.babraham.ac.uk/projects/fastqc/>). Since all the samples represented the interaction of two organisms, the genome of *C. rosea* was concatenated with the one of either *B. cinerea* or *F. graminearum*, creating two "combined genomes" (Cr-Fg and Cr-Bc), and the same was done with the annotations in .gff format. Reads from the *C. rosea*-*B. cinerea* interaction were aligned to the Cr-Bc genome, whereas reads from the *C. rosea*-*F. graminearum* interaction were aligned to the Cr-Fg. The chosen aligner was STAR v.2.7.5c (132), with default options, and the count tables were then generated through featureCounts v.2.0.1 (133). Finally, the differential expression analysis was done with DESeq2 v.1.28.1 (134), where an FDR of <0.05 in combination with a log₂FC of >1.5 or <-1.5 was considered to define differentially expressed genes (DEGs). Enrichment in gene ontology (GO) terms of DEGs was determined through Fisher tests integrated in the BLAST2GO suite, with an FDR threshold of 0.05.

(iii) Mapping of sRNAs. sRNA reads were trimmed with bbduk v.38.86 (131) with the same options used for mRNA read trimming, and successful cleaning and adapter removal was verified with fastqc v.0.11.9. The program SortMeRna v.4.2.0 (135) was used to remove structural sRNA (rRNA, tRNA, snRNA, and snoRNA) from the reads, and sequences within the length range of 18 to 32 bp were isolated with the command reformat.sh of the BBTtools suite (131). The database of structural RNAs used for SortMeRna consisted

in the rRNA sequences of the SILVA database (136), while snRNA, tRNA, and snoRNA sequences were downloaded from the NRDR database (137). After filtering, the sRNA reads were mapped to the Cr-Bc and Cr-Fg genomes with STAR, with the following options recommended for sRNA mapping: STAR -genomeDir index/-readFilesIn read1.fq read2.fq -outFileNamePrefix prefix -outFilterMismatchNoverLmax 0.05 -outFilterMatchNmin 16 -outFilterScoreMinOverLread 0 -outFilterMatchNminOverLread 0 -alignIntronMax 1 -alignEndsType EndToEnd. For the STAR default option, reads with good mapping results on more than 20 different loci were considered “not mapped.”

Untranslated regions (UTRs) and introns were added to the .gff files of the genomes through “add_utrs_to_gff” (https://github.com/dpryan79/Answers/tree/master/bioinfoSE_3181) and GenomeTools with the “-addintrons” option (138), respectively. Promoters were also added through an *ad hoc* Python script (https://github.com/EdoardoPiombo/promoter_extractor), considering promoters to be composed of the first 1,000 bases upstream of a gene or of all the bases until the end of the precedent gene. Introns, promoters, and UTRs were all considered when featureCounts was used to generate the count tables.

(iv) Prediction of miRNA-like RNAs and subsequent analyses. Putative miRNAs were predicted with mirdeep2 v.2.0.1.2 (139). The miRbase database (140), as well as all the fungal miRNA sequences from RNAcentral (141), were used to provide reference sequences from other species. To ensure the novelty of newly detected miRNAs, BLAST was used to compare them to the fungal miRNAs identified in several other studies, plus all the fungal miRNAs available in RNAcentral, requiring 95% minimum identity and query coverage (25, 33, 141–145). Nonstructural sRNA reads, previously mapped to the genomes with STAR, were counted with featureCounts, and the differentially expressed miRNAs were identified with DESeq2, with the same thresholds used for DEG analysis.

The sRNA_toolbox (146) was used to predict putative targets for the identified miRNAs. The prediction was carried out with the animal-based tools PITA, Miranda, TargetSpy (147–149), and simple seed analysis and with the plant-based tools psRobot, TAPIR FASTA, and TAPIR RNAhybrid (150, 151). Target-miRNA couples identified by at least three animal-based tools or two plant-based ones were retained for the following analyses. Predicted targets were retained only when they were significantly expressed (FDR < 0.05) with a $\log_2FC > 1.0$ opposite to the miRNA. Putative targets of downregulated miRNAs were therefore considered only when they were overexpressed. The predicted targets present in double copy in their genome were then removed from the analysis. Repetitive elements in the genome of *C. rosea* were predicted according to the guidelines for basic repeat library construction (http://weatherby.genetics.utah.edu/MAKER/wiki/index.php/Repeat_Library_Construction-Basic), using all fungal transposons in RepetDB as known transposons (152), and putative miRNA targets within 700 bp from any *C. rosea* transposon were removed from the analysis.

(v) Validation of miRNA-expression through stem-loop RT-qPCR. miRNA specific stem-loop RT-qPCR primers (see Table S1B) were designed as described previously (153). Stem-loop RT primers (1 μ M) were denatured at 65°C for 5 min and immediately transferred to ice. For each miRNA RT reaction, a “no RNA” master mix was prepared with 0.5 μ l of 10 mM dNTP (Thermo Scientific, Waltham, MA), 5 \times SSIV buffer, 2 μ l of 0.1 M dithiothreitol, 0.1 μ l of RiboLock RNase inhibitor (40 U/ μ l), 0.25 μ l of SSIII reverse transcriptase (Invitrogen, Waltham, MA), 1 μ l of denatured stem-loop RT primer, and 1 μ l of 5 μ M reverse primer of *C. rosea* actin (*act*) reference gene. Next, 10 ng of RNA template used for next-generation sequencing analysis was added into respective reactions. The tubes were then incubated in a thermal cycler at 16°C for 30 min, followed by 60 cycles of pulsed RT at 30°C for 30 s, 42°C for 30 s, and 50°C for 1 s and then enzyme inactivation at 85°C for 5 min. Quantitative PCR was performed using DyNAmo Flash SYBR green kit (Thermo Scientific, Waltham, MA) according to the manufacturer’s instructions. The C_T values of miRNA were normalized to that of *act* to be used for quantification using the $\Delta\Delta C_T$ method (154).

Data availability. The raw sequencing data were submitted to ENA in under BioProject accession number PRJEB43636. This project contains both the transcriptome and the sRNA sequencing data for each of the samples.

SUPPLEMENTAL MATERIAL

Supplemental material is available online only.

SUPPLEMENTAL FILE 1, XLSX file, 0.02 MB.

SUPPLEMENTAL FILE 2, XLSX file, 1.9 MB.

SUPPLEMENTAL FILE 3, XLSX file, 0.4 MB.

SUPPLEMENTAL FILE 4, XLSX file, 0.1 MB.

SUPPLEMENTAL FILE 5, XLSX file, 0.2 MB.

SUPPLEMENTAL FILE 6, PDF file, 1.7 MB.

ACKNOWLEDGMENTS

This study was financially supported by the Department of Forest Mycology and Plant Pathology; the Swedish Research Council for Environment, Agricultural Sciences, and Spatial Planning (FORMAS; grant 2018-01420); and the Carl Tryggers Stiftelse för Vetenskaplig Forskning (CTS 19:82). M.K. acknowledges the SLU Centre for Biological Control at the Swedish University of Agricultural Sciences. R.R.V. is supported by FORMAS (2019-01316), Carl Tryggers Stiftelse för Vetenskaplig Forskning (CTS 20:464), and The Crafoord Foundation (20200818).

REFERENCES

- Ghildiyal M, Zamore PD. 2009. Small silencing RNAs: an expanding universe. *Nat Rev Genet* 10:94–108. <https://doi.org/10.1038/nrg2504>.
- Hannon GJ. 2002. RNA interference. *Nature* 418:244–251. <https://doi.org/10.1038/418244a>.
- Huang CY, Wang H, Hu P, Hamby R, Jin H. 2019. Small RNAs: big players in plant-microbe interactions. *Cell Host Microbe* 26:173–182. <https://doi.org/10.1016/j.chom.2019.07.021>.
- Malone CD, Hannon GJ. 2009. Small RNAs as guardians of the genome. *Cell* 136:656–668. <https://doi.org/10.1016/j.cell.2009.01.045>.
- Van Wolfswinkel JC, Ketting RF. 2010. The role of small noncoding RNAs in genome stability and chromatin organization. *J Cell Sci* 123:1825–1839. <https://doi.org/10.1242/jcs.061713>.
- Lee HC, Li L, Gu W, Xue Z, Crosthwaite SK, Pertsemliadis A, Lewis ZA, Freitag M, Selker EU, Mello CC, Liu Y. 2010. Diverse pathways generate microRNA-like RNAs and Dicer-independent small interfering RNAs in fungi. *Mol Cell* 38:803–814. <https://doi.org/10.1016/j.molcel.2010.04.005>.
- Nicolás FE, Ruiz-Vázquez RM. 2013. Functional diversity of RNAi-associated sRNAs in fungi. *Int J Mol Sci* 14:15348–15360. <https://doi.org/10.3390/ijms140815348>.
- Torres-Martínez S, Ruiz-Vázquez RM. 2017. The RNAi universe in fungi: a varied landscape of small RNAs and biological functions. *Annu Rev Microbiol* 71:371–391. <https://doi.org/10.1146/annurev-micro-090816-093352>.
- Romano N, Macino G. 1992. Quelling: transient inactivation of gene expression in *Neurospora crassa* by transformation with homologous sequences. *Mol Microbiol* 6:3343–3353. <https://doi.org/10.1111/j.1365-2958.1992.tb02202.x>.
- Aramayo R, Metzberg RL. 1996. Meiotic transvection in fungi. *Cell* 86:103–113. [https://doi.org/10.1016/S0092-8674\(00\)80081-1](https://doi.org/10.1016/S0092-8674(00)80081-1).
- Shiu PKT, Raju NB, Zickler D, Metzberg RL. 2001. Meiotic silencing by unpaired DNA. *Cell* 107:905–916. [https://doi.org/10.1016/S0092-8674\(01\)00609-2](https://doi.org/10.1016/S0092-8674(01)00609-2).
- Hammond TM, Keller NP. 2005. RNA silencing in *Aspergillus nidulans* is independent of RNA-dependent RNA polymerases. *Genetics* 169:607–617. <https://doi.org/10.1534/genetics.104.035964>.
- Janbon G, Maeng S, Yang DH, Ko YJ, Jung KW, Moyrand F, Floyd A, Heitman J, Bahn YS. 2010. Characterizing the role of RNA silencing components in *Cryptococcus neoformans*. *Fungal Genet Biol* 47:1070–1080. <https://doi.org/10.1016/j.fgb.2010.10.005>.
- Wang X, Wang P, Sun S, Darwiche S, Idrum A, Heitman J. 2012. Transgene induced co-suppression during vegetative growth in *Cryptococcus neoformans*. *PLoS Genet* 8:e1002885. <https://doi.org/10.1371/journal.pgen.1002885>.
- Son H, Min K, Lee J, Raju NB, Lee YW. 2011. Meiotic silencing in the homothallic fungus *Gibberella zeae*. *Fungal Biol* 115:1290–1302. <https://doi.org/10.1016/j.funbio.2011.09.006>.
- Kadotani N, Nakayashiki H, Tosa Y, Mayama S. 2003. RNA silencing in the phytopathogenic fungus *Magnaporthe oryzae*. *Mol Plant Microbe Interact* 16:769–776. <https://doi.org/10.1094/MPMI.2003.16.9.769>.
- Murata T, Kadotani N, Yamaguchi M, Tosa Y, Mayama S, Nakayashiki H. 2007. siRNA-dependent and-independent posttranscriptional cosuppression of the LTR-retrotransposon MAGGY in the phytopathogenic fungus *Magnaporthe oryzae*. *Nucleic Acids Res* 35:5987–5994. <https://doi.org/10.1093/nar/gkm646>.
- De Haro JP, Calo S, Cervantes M, Nicolás FE, Torres-Martínez S, Ruiz-Vázquez RM. 2009. A single dicer gene is required for efficient gene silencing associated with two classes of small antisense RNAs in *Mucor circinelloides*. *Eukaryot Cell* 8:1486–1497. <https://doi.org/10.1128/EC.00191-09>.
- Nicolás FE, Moxon S, de Haro JP, Calo S, Grigoriev IV, Torres-Martínez S, Moulton V, Ruiz-Vázquez RM, Dalmay T. 2010. Endogenous short RNAs generated by Dicer 2 and RNA-dependent RNA polymerase 1 regulate mRNAs in the basal fungus *Mucor circinelloides*. *Nucleic Acids Res* 38:5535–5541. <https://doi.org/10.1093/nar/gkq301>.
- Carreras-Villaseñor N, Esquivel-Naranjo EU, Villalobos-Escobedo JM, Abreu-Goodger C, Herrera-Estrella A. 2013. The RNAi machinery regulates growth and development in the filamentous fungus *Trichoderma atroviride*. *Mol Microbiol* 89:96–116. <https://doi.org/10.1111/mmi.12261>.
- Laurie JD, Linning R, Bakkeren G. 2008. Hallmarks of RNA silencing are found in the smut fungus *Ustilago hordei* but not in its close relative *Ustilago maydis*. *Curr Genet* 53:49–58. <https://doi.org/10.1007/s00294-007-0165-7>.
- Drinnenberg IA, Weinberg DE, Xie KT, Mower JP, Wolfe KH, Fink GR, Bartel DP. 2009. RNAi in budding yeast. *Science* 326:544–550. <https://doi.org/10.1126/science.1176945>.
- Dang Y, Yang Q, Xue Z, Liu Y. 2011. RNA interference in fungi: pathways, functions, and applications. *Eukaryot Cell* 10:1148–1155. <https://doi.org/10.1128/EC.05109-11>.
- Bai Y, Lan F, Yang W, Zhang F, Yang K, Li Z, Gao P, Wang S. 2015. SRNA profiling in *Aspergillus flavus* reveals differentially expressed miRNA-like RNAs response to water activity and temperature. *Fungal Genet Biol* 81:113–119. <https://doi.org/10.1016/j.fgb.2015.03.004>.
- Kang K, Zhong J, Jiang L, Liu G, Gou CY, Wu Q, Wang Y, Luo J, Gou D. 2013. Identification of microRNA-like RNAs in the filamentous fungus *Trichoderma reesei* by Solexa sequencing. *PLoS One* 8:e76288. <https://doi.org/10.1371/journal.pone.0076288>.
- Lau SKP, Chow WN, Wong AYP, Yeung JMY, Bao J, Zhang N, Lok S, Woo PCY, Yuen KY. 2013. Identification of microRNA-like RNAs in mycelial and yeast phases of the thermal dimorphic fungus *Penicillium marneffei*. *PLoS Negl Trop Dis* 7:e2398. <https://doi.org/10.1371/journal.pntd.0002398>.
- Lin YL, Ma LT, Lee YR, Lin SS, Wang SY, Chang TT, Shaw JF, Li WH, Chu FH. 2015. MicroRNA-like small RNAs prediction in the development of *Antrodia cinnamomea*. *PLoS One* 10:e0123245. <https://doi.org/10.1371/journal.pone.0123245>.
- Lin R, He L, He J, Qin P, Wang Y, Deng Q, Yang X, Li S, Wang S, Wang W, Liu H, Li P, Zheng A. 2016. Comprehensive analysis of microRNA-seq and target mRNAs of rice sheath blight pathogen provides new insights into pathogenic regulatory mechanisms. *DNA Res* 23:415–425. <https://doi.org/10.1093/dnares/dsw024>.
- Liu T, Hu J, Zuo Y, Jin Y, Hou J. 2016. Identification of microRNA-like RNAs from *Curvularia lunata* associated with maize leaf spot by bioinformatics analysis and deep sequencing. *Mol Genet Genomics* 291:587–596. <https://doi.org/10.1007/s00438-015-1128-1>.
- Mueth NA, Ramachandran SR, Hulbert SH. 2015. Small RNAs from the wheat stripe rust fungus (*Puccinia striiformis* f.sp. tritici). *BMC Genomics* 16:718–716. <https://doi.org/10.1186/s12864-015-1895-4>.
- Nunes CC, Gowda M, Sailsbery J, Xue M, Chen F, Brown DE, Oh YY, Mitchell TK, Dean RA. 2011. Diverse and tissue-enriched small RNAs in the plant pathogenic fungus *Magnaporthe oryzae*. *BMC Genomics* 12:288–220. <https://doi.org/10.1186/1471-2164-12-288>.
- Raman V, Simon SA, Romag A, Demirci F, Mathioni SM, Zhai J, Meyers BC, Donofrio NM. 2013. Physiological stressors and invasive plant infections alter the small RNA transcriptome of the rice blast fungus *Magnaporthe oryzae*. *BMC Genomics* 14:326–318. <https://doi.org/10.1186/1471-2164-14-326>.
- Zhou Q, Wang Z, Zhang J, Meng H, Huang B. 2012. Genome-wide identification and profiling of microRNA-like RNAs from *Metarhizium anisopliae* during development. *Fungal Biol* 116:1156–1162. <https://doi.org/10.1016/j.funbio.2012.09.001>.
- Zhou J, Fu Y, Xie J, Li B, Jiang D, Li G, Cheng J. 2012. Identification of microRNA-like RNAs in a plant pathogenic fungus *Sclerotinia sclerotiorum* by high-throughput sequencing. *Mol Genet Genomics* 287:275–282. <https://doi.org/10.1007/s00438-012-0678-8>.
- Weiberg A, Wang M, Lin FM, Zhao H, Zhang Z, Kaloshian I, Da Huang H, Jin H. 2013. Fungal small RNAs suppress plant immunity by hijacking host RNA interference pathways. *Science* 342:118–123. <https://doi.org/10.1126/science.1239705>.
- Weiberg A, Jin H. 2015. Small RNAs—the secret agents in the plant-pathogen interactions. *Curr Opin Plant Biol* 26:87–94. <https://doi.org/10.1016/j.pbi.2015.05.033>.
- Chaloner T, van Kan JAL, Grant-Downton RT. 2016. RNA ‘information warfare’ in pathogenic and mutualistic interactions. *Trends Plant Sci* 21:738–748. <https://doi.org/10.1016/j.tplants.2016.05.008>.
- Wang M, Weiberg A, Lin FM, Thomma BPHJ, Huang H, Da JH. 2016. Bidirectional cross-kingdom RNAi and fungal uptake of external RNAs confer plant protection. *Nat Plants* 2:1–10.
- Zhang T, Zhao YL, Zhao JH, Wang S, Jin Y, Chen ZQ, Fang YY, Hua CL, Ding SW, Guo HS. 2016. Cotton plants export microRNAs to inhibit virulence gene expression in a fungal pathogen. *Nat Plants* 2:1–6.
- Cui C, Wang Y, Liu J, Zhao J, Sun P, Wang S. 2019. A fungal pathogen deploys a small silencing RNA that attenuates mosquito immunity and facilitates infection. *Nat Commun* 10:4298–4210. <https://doi.org/10.1038/s41467-019-12323-1>.
- Karlsson M, Durling MB, Choi J, Kosawang C, Lackner G, Tzelepis GD, Nygren K, Dubey MK, Kamou N, Levasseur A, Zapparata A, Wang J, Amby DB, Jensen B, Sarrocco S, Panteris E, Lagopodi AL, Pöggeler S, Vannacci G, Collinge DB, Hoffmeister D, Henrissat B, Lee YH, Jensen DF. 2015. Insights on the evolution of mycoparasitism from the genome of *clonostachys rosea*. *Genome Biol Evol* 7:465–480. <https://doi.org/10.1093/gbe/evu292>.
- Iqbal M, Dubey M, Mcewan K, Menzel U, Franko MA, Viketoft M, Jensen DF, Karlsson M. 2018. Evaluation of *clonostachys rosea* for control of

- plant-parasitic nematodes in soil and in roots of carrot and wheat. *Phytopathology* 108:52–59. <https://doi.org/10.1094/PHYTO-03-17-0091-R>.
43. Dubey M, Véléz H, Broberg M, Jensen DF, Karlsson M. 2020. LysM proteins regulate fungal development and contribute to hyphal protection and biocontrol traits in *Clonostachys rosea*. *Front Microbiol* 11:679. <https://doi.org/10.3389/fmicb.2020.00679>.
 44. Tzelepis G, Dubey M, Jensen DF, Karlsson M. 2015. Identifying glycoside hydrolase family 18 genes in the mycoparasitic fungal species *Clonostachys rosea*. *Microbiology (Reading)* 161:1407–1419. <https://doi.org/10.1099/mic.0.000096>.
 45. Dubey MK, Jensen DF, Karlsson M. 2014. Hydrophobins are required for conidial hydrophobicity and plant root colonization in the fungal biocontrol agent *Clonostachys rosea*. *BMC Microbiol* 14:18–14. <https://doi.org/10.1186/1471-2180-14-18>.
 46. Bin Sun Z, Sun MH, Li SD. 2015. Identification of mycoparasitism-related genes in *Clonostachys rosea* 67-1 active against *Sclerotinia sclerotiorum*. *Sci Rep* 5:18169. <https://doi.org/10.1038/srep18169>.
 47. Demissie ZA, Foote SJ, Tan Y, Loewen MC. 2018. Profiling of the transcriptomic responses of *Clonostachys rosea* upon treatment with *Fusarium graminearum* secretome. *Front Microbiol* 9:1061. <https://doi.org/10.3389/fmicb.2018.01061>.
 48. Demissie ZA, Witte T, Robinson KA, Sproule A, Foote SJ, Johnston A, Harris LJ, Overy DP, Loewen MC. 2020. Transcriptomic and exometabolic profiling reveals antagonistic and defensive modes of *Clonostachys rosea* action against *Fusarium graminearum*. *Mol Plant Microbe Interact* 33:842–858. <https://doi.org/10.1094/MPMI-11-19-0310-R>.
 49. Nygren K, Dubey M, Zapparata A, Iqbal M, Tzelepis GD, Durling MB, Jensen DF, Karlsson M. 2018. The mycoparasitic fungus *Clonostachys rosea* responds with both common and specific gene expression during interspecific interactions with fungal prey. *Evol Appl* 11:931–949. <https://doi.org/10.1111/eva.12609>.
 50. Fatema U, Broberg A, Jensen DF, Karlsson M, Dubey M. 2018. Functional analysis of polyketide synthase genes in the biocontrol fungus *Clonostachys rosea*. *Sci Rep* 8:15009–15017. <https://doi.org/10.1038/s41598-018-33391-1>.
 51. Dubey M, Jensen D, Karlsson M. 2016. The ABC transporter ABCG29 is involved in H2O2 tolerance and biocontrol traits in the fungus *Clonostachys rosea*. *Mol Genet Genomics* 291:677–686. <https://doi.org/10.1007/s00438-015-1139-y>.
 52. Kamou NN, Dubey M, Tzelepis G, Menexes G, Papadakis EN, Karlsson M, Lagopodi AL, Jensen DF. 2016. Investigating the compatibility of the biocontrol agent *Clonostachys rosea* IK726 with prodigiosin-producing *Serratia rubidua* S55 and phenazine-producing *Pseudomonas chlororaphis* ToZa7. *Arch Microbiol* 198:369–377. <https://doi.org/10.1007/s00203-016-1198-4>.
 53. Dubey MK, Jensen DF, Karlsson M. 2014. An ATP-binding cassette pleiotropic drug transporter protein is required for xenobiotic tolerance and antagonism in the fungal biocontrol agent *Clonostachys rosea*. *Mol Plant Microbe Interact* 27:725–732. <https://doi.org/10.1094/MPMI-12-13-0365-R>.
 54. Iqbal M, Broberg M, Haarith D, Broberg A, Bushley KE, Brandström Durling M, Viketoft M, Funck Jensen D, Dubey M, Karlsson M. 2020. Natural variation of root lesion nematode antagonism in the biocontrol fungus *Clonostachys rosea* and identification of biocontrol factors through genome-wide association mapping. *Evol Appl* 13:2264–2283. <https://doi.org/10.1111/eva.13001>.
 55. Broberg M, Dubey M, Sun MH, Ihrmark K, Schroers HJ, Li SD, Jensen DF, Durling MB, Karlsson M. 2018. Out in the cold: identification of genomic regions associated with cold tolerance in the biocontrol fungus *Clonostachys rosea* through genome-wide association mapping. *Front Microbiol* 9:2844. <https://doi.org/10.3389/fmicb.2018.02844>.
 56. Meng J, Wang X, Xu D, Fu X, Zhang X, Lai D, Zhou L, Zhang G. 2016. Sorbicillinoids from fungi and their bioactivities. *Molecules* 21:715. <https://doi.org/10.3390/molecules21060715>.
 57. Brown DW, Lee SH, Kim LH, Ryu JG, Lee S, Seo Y, Kim YH, Busman M, Yun SH, Proctor RH, Lee T. 2015. Identification of a 12-gene fusaric acid biosynthetic gene cluster in *Fusarium* species through comparative and functional genomics. *Mol Plant Microbe Interact* 28:319–332. <https://doi.org/10.1094/MPMI-09-14-0264-R>.
 58. Crutcher FK, Liu J, Puckhaber LS, Stipanovic RD, Bell AA, Nichols RL. 2015. FUBT, a putative MFS transporter, promotes secretion of fusaric acid in the cotton pathogen *Fusarium oxysporum* f.sp. vasinfectum. *Microbiology (Reading)* 161:875–883. <https://doi.org/10.1099/mic.0.000043>.
 59. Reeves CD, Hu Z, Reid R, Kealey JT. 2008. Genes for the biosynthesis of the fungal polyketides hypothemycin from *Hypomyces subiculosus* and radicicol from *Pochonia chlamydosporia*. *Appl Environ Microbiol* 74: 5121–5129. <https://doi.org/10.1128/AEM.00478-08>.
 60. Yu J, Bhatnagar D, Cleveland TE. 2004. Completed sequence of aflatoxin pathway gene cluster in *Aspergillus parasiticus*. *FEBS Lett* 564:126–130. [https://doi.org/10.1016/S0014-5793\(04\)00327-8](https://doi.org/10.1016/S0014-5793(04)00327-8).
 61. Keller NP. 2019. Fungal secondary metabolism: regulation, function, and drug discovery. *Nat Rev Microbiol* 17:167–180. <https://doi.org/10.1038/s41579-018-0121-1>.
 62. Derntl C, Rassinger A, Srebotnik E, Mach RL, Mach-Aigner AR. 2016. Identification of the main regulator responsible for synthesis of the typical yellow pigment produced by *Trichoderma reesei*. *Appl Environ Microbiol* 82:6247–6257. <https://doi.org/10.1128/AEM.01408-16>.
 63. Derntl C, Guzmán-Chávez F, Mello-de-Sousa TM, Busse H-J, Driessen AJM, Mach RL, Mach-Aigner AR. 2017. *In vivo* study of the sorbicillinoid gene cluster in *Trichoderma reesei*. *Front Microbiol* 8:2037. <https://doi.org/10.3389/fmicb.2017.02037>.
 64. Boylan MT, Mirabito PM, Willett CE, Zimmerman CR, Timberlake WE. 1987. Isolation and physical characterization of three essential conidiation genes from *Aspergillus nidulans*. *Mol Cell Biol* 7:3113–3118. <https://doi.org/10.1128/mcb.7.9.3113-3118.1987>.
 65. Adams TH, Timberlake WE. 1990. Developmental repression of growth and gene expression in *Aspergillus*. *Proc Natl Acad Sci U S A* 87: 5405–5409. <https://doi.org/10.1073/pnas.87.14.5405>.
 66. Hindley J, Phear G, Stein M, Beach D. 1987. Sucl+ encodes a predicted 13-kilodalton protein that is essential for cell viability and is directly involved in the division cycle of *Schizosaccharomyces pombe*. *Mol Cell Biol* 7:504–511. <https://doi.org/10.1128/mcb.7.1.504-511.1987>.
 67. Finkel JS, Xu W, Huang D, Hill EM, Desai JV, Woolford CA, Nett JE, Taff H, Norice CT, Andes DR, Lanni F, Mitchell AP. 2012. Portrait of *Candida albicans* adherence regulators. *PLoS Pathog* 8:e1002525. <https://doi.org/10.1371/journal.ppat.1002525>.
 68. Ridenour JB, Bluhm BH. 2014. The HAP complex in *Fusarium verticillioides* is a key regulator of growth, morphogenesis, secondary metabolism, and pathogenesis. *Fungal Genet Biol* 69:52–64. <https://doi.org/10.1016/j.fgb.2014.05.003>.
 69. Son H, Park AR, Lim JY, Shin C, Lee YW. 2017. Genome-wide exonic small interference RNA-mediated gene silencing regulates sexual reproduction in the homothallic fungus *Fusarium graminearum*. *PLoS Genet* 13: e1006595. <https://doi.org/10.1371/journal.pgen.1006595>.
 70. Liu L, Wang Q, Zhang X, Liu J, Zhang Y, Pan H. 2018. *Sams2*, a gene encoding GATA transcription factor, is required for appressorium formation and chromosome segregation in *Sclerotinia sclerotiorum*. *Front Microbiol* 9:3031. <https://doi.org/10.3389/fmicb.2018.03031>.
 71. Hirayama S, Sugiura R, Lu Y, Maeda T, Kawagishi K, Yokoyama M, Tohda H, Giga-Hama Y, Shuntoh H, Kuno T. 2003. Zinc finger protein Prz1 regulates Ca²⁺ but not Cl⁻ homeostasis in fission yeast: identification of distinct branches of calcineurin signaling pathway in fission yeast. *J Biol Chem* 278:18078–18084. <https://doi.org/10.1074/jbc.M212900200>.
 72. Ryan DP, Owen-Hughes T. 2011. Snf2-family proteins: chromatin remodelers for any occasion. *Curr Opin Chem Biol* 15:649–656. <https://doi.org/10.1016/j.cbpa.2011.07.022>.
 73. Baccile JA, Spraker JE, Le HH, Brandenburger E, Gomez C, Bok JW, MacHeleidt J, Brakhage AA, Hoffmeister D, Keller NP, Schroeder FC. 2016. Plant-like biosynthesis of isoquinoline alkaloids in *Aspergillus fumigatus*. *Nat Chem Biol* 12:419–424. <https://doi.org/10.1038/nchembio.2061>.
 74. Macheleidt J, Scherlach K, Neuwirth T, Schmidt-Heck W, Straßburger M, Spraker J, Baccile JA, Schroeder FC, Keller NP, Hertweck C, Heinekamp T, Brakhage AA. 2015. Transcriptome analysis of cyclic AMP-dependent protein kinase A-regulated genes reveals the production of the novel natural compound fumipyrrole by *Aspergillus fumigatus*. *Mol Microbiol* 96:148–162. <https://doi.org/10.1111/mmi.12926>.
 75. Zhai MM, Qi FM, Li J, Jiang CX, Hou Y, Shi YP, Di DL, Zhang JW, Wu QX. 2016. Isolation of secondary metabolites from the soil-derived fungus *Clonostachys rosea* YRS-06, a biological control agent, and evaluation of antibacterial activity. *J Agric Food Chem* 64:2298–2306. <https://doi.org/10.1021/acs.jafc.6b00556>.
 76. Seidl V, Huemer B, Seiboth B, Kubicek CP. 2005. A complete survey of *Trichoderma* chitinases reveals three distinct subgroups of family 18 chitinases. *FEBS J* 272:5923–5939. <https://doi.org/10.1111/j.1742-4658.2005.04994.x>.
 77. Karlsson M, Stenlid J. 2008. Comparative evolutionary histories of the fungal chitinase gene family reveal non-random size expansions and contractions due to adaptive natural selection. *Evol Bioinforma Online* 4:47–60.
 78. Steindorff AS, Ramada MHS, Coelho ASG, Miller RNG, Pappas GJ, Ulhoa CJ, Noronha EF. 2014. Identification of mycoparasitism-related genes against the phytopathogen *Sclerotinia sclerotiorum* through transcriptome and expression profile analysis in *Trichoderma harzianum*. *BMC Genomics* 15:204–140. <https://doi.org/10.1186/1471-2164-15-204>.

79. Broberg M, Dubey M, Iqbal M, Gudmundsson M, Ihrmark K, Schroers HJ, Funck Jensen D, Brandström Durling M, Karlsson M. 2021. Comparative genomics highlights the importance of drug efflux transporters during evolution of mycoparasitism in *Clonostachys* subgenus *bionectria* (Fungi, Ascomycota, Hypocreales). *Evol Appl* 14:476–497. <https://doi.org/10.1111/eva.13134>.
80. Ridenour JB, Smith JE, Bluhm BH. 2016. The HAP complex governs fumonisin biosynthesis and maize kernel pathogenesis in *Fusarium verticillioides*. *J Food Prot* 79:1498–1507. <https://doi.org/10.4315/0362-028XJFP-15-596>.
81. Son H, Seo YS, Min K, Park AR, Lee J, Jin JM, Lin Y, Cao P, Hong SY, Kim EK, Lee SH, Cho A, Lee S, Kim MG, Kim Y, Kim JE, Kim JC, Choi GJ, Yun SH, Lim JY, Kim M, Lee YH, Choi YD, Lee YW. 2011. A phenome-based functional analysis of transcription factors in the cereal head blight fungus, *Fusarium graminearum*. *PLoS Pathog* 7:e1002310. <https://doi.org/10.1371/journal.ppat.1002310>.
82. Seong K, Hou Z, Tracy M, Kistler HC, Xu JR. 2005. Random insertional mutagenesis identifies genes associated with virulence in the wheat scab fungus *Fusarium graminearum*. *Phytopathology* 95:744–750. <https://doi.org/10.1094/PHYTO-95-0744>.
83. Oh M, Son H, Choi GJ, Lee C, Kim JC, Kim H, Lee YW. 2016. Transcription factor ART1 mediates starch hydrolysis and mycotoxin production in *Fusarium graminearum* and *F. verticillioides*. *Mol Plant Pathol* 17:755–768. <https://doi.org/10.1111/mpp.12328>.
84. Gourgues M, Brunet-Simon A, Lebrun MH, Levis C. 2004. The tetraspanin BcPls1 is required for appressorium-mediated penetration of *Botrytis cinerea* into host plant leaves. *Mol Microbiol* 51:619–629. <https://doi.org/10.1046/j.1365-2958.2003.03866.x>.
85. Schumacher J, Kokkelink L, Huesmann C, Jimenez-Teja D, Collado IG, Barakat R, Tudzynski P, Tudzynski B. 2008. The cAMP-dependent signaling pathway and its role in conidial germination, growth, and virulence of the gray mold *Botrytis cinerea*. *Mol Plant Microbe Interact* 21:1443–1459. <https://doi.org/10.1094/MPMI-21-11-1443>.
86. Siegmund U, Marschall R, Tudzynski P. 2015. BcNoxD, a putative ER protein, is a new component of the NADPH oxidase complex in *Botrytis cinerea*. *Mol Microbiol* 95:988–1005. <https://doi.org/10.1111/mmi.12869>.
87. Schamber A, Lerocq M, Diwo J, Mendgen K, Hahn M. 2010. The role of mitogen-activated protein (MAP) kinase signaling components and the Ste12 transcription factor in germination and pathogenicity of *Botrytis cinerea*. *Mol Plant Pathol* 11:105–119. <https://doi.org/10.1111/j.1364-3703.2009.00579.x>.
88. Kim Y, Kim H, Son H, Choi GJ, Kim JC, Lee YW. 2014. MYT3, a Myb-like transcription factor, affects fungal development and pathogenicity of *Fusarium graminearum*. *PLoS One* 9:e94359. <https://doi.org/10.1371/journal.pone.0094359>.
89. Jonkers W, Xayamongkhon H, Haas M, Olivain C, van der Does HC, Broz K, Rep M, Alabouvette C, Steinberg C, Kistler HC. 2014. EBR1 genomic expansion and its role in virulence of *Fusarium* species. *Environ Microbiol* 16:1982–2003. <https://doi.org/10.1111/1462-2920.12331>.
90. Zhao C, Waalwijk C, De Wit PJGM, Van Der Lee T, Tang D. 2011. EBR1, a novel Zn2Cys6 transcription factor, affects virulence and apical dominance of the hyphal tip in *Fusarium graminearum*. *Mol Plant Microbe Interact* 24:1407–1418. <https://doi.org/10.1094/MPMI-06-11-0158>.
91. Dufresne M, van der Lee T, Ben Mbarek S, Xu X, Zhang X, Liu T, Waalwijk C, Zhang W, Kema GHJ, Daboussi M-J. 2008. Transposon-tagging identifies novel pathogenicity genes in *Fusarium graminearum*. *Fungal Genet Biol* 45:1552–1561. <https://doi.org/10.1016/j.fgb.2008.09.004>.
92. Zhu Q, Sun L, Lian J, Gao X, Zhao L, Ding M, Li J, Liang Y. 2016. The phospholipase C (FgPLC1) is involved in regulation of development, pathogenicity, and stress responses in *Fusarium graminearum*. *Fungal Genet Biol* 97:1–9. <https://doi.org/10.1016/j.fgb.2016.10.004>.
93. Cao SN, Yuan Y, Qin YH, Zhang MZ, de Figueiredo P, Li GH, Qin QM. 2018. The pre-rRNA processing factor Nop53 regulates fungal development and pathogenesis via mediating production of reactive oxygen species. *Environ Microbiol* 20:1531–1549. <https://doi.org/10.1111/1462-2920.14082>.
94. Li H, Tian S, Qin G. 2019. NADPH oxidase is crucial for the cellular redox homeostasis in fungal pathogen *Botrytis cinerea*. *Mol Plant Microbe Interact* 32:1508–1516. <https://doi.org/10.1094/MPMI-05-19-0124-R>.
95. Hevia MA, Canessa P, Müller-Esparza H, Larrondo LF. 2015. A circadian oscillator in the fungus *Botrytis cinerea* regulates virulence when infecting *Arabidopsis thaliana*. *Proc Natl Acad Sci U S A* 112:8744–8749. <https://doi.org/10.1073/pnas.1508432112>.
96. Schumacher J, Pradier JM, Simon A, Traeger S, Moraga J, Collado IG, Viaud M, Tudzynski B. 2012. Natural variation in the VELVET gene *bcvel1* affects virulence and light-dependent differentiation in *Botrytis cinerea*. *PLoS One* 7:e47840. <https://doi.org/10.1371/journal.pone.0047840>.
97. Li J, Mu W, Veluchamy S, Liu Y, Zhang Y, Pan H, Rollins JA. 2018. The GATA-type IVb zinc-finger transcription factor SsNsd1 regulates asexual–sexual development and appressoria formation in *Sclerotinia sclerotiorum*. *Mol Plant Pathol* 19:1679–1689. <https://doi.org/10.1111/mpp.12651>.
98. Bi K, Scalschi L, Jaiswal N, Mengiste T, Fried R, Sanz AB, Arroyo J, Zhu W, Masrati G, Sharon A. 2021. The *Botrytis cinerea* Crh transglycosylase is a cytoplasmic effector triggering plant cell death and defense response. *Nat Commun* 12:2166. <https://doi.org/10.1038/s41467-021-22436-1>.
99. Cui Z, Ding Z, Yang X, Wang K, Zhu T. 2009. Gene disruption and characterization of a class V chitin synthase in *Botrytis cinerea*. *Can J Microbiol* 55:1267–1274. <https://doi.org/10.1139/w09-076>.
100. Cui Z, Wang Y, Lei N, Wang K, Zhu T. 2013. *Botrytis cinerea* chitin synthase BcChsVI is required for normal growth and pathogenicity. *Curr Genet* 59:119–128. <https://doi.org/10.1007/s00294-013-0393-y>.
101. Morcx S, Kunz C, Choquer M, Assie S, Blondet E, Simond-Côte E, Gajek K, Chapeland-Leclerc F, Expert D, Soulie MC. 2013. Disruption of Bcchs4, Bcchs6, or Bcchs7 chitin synthase genes in *Botrytis cinerea* and the essential role of class VI chitin synthase (Bcchs6). *Fungal Genet Biol* 52:1–8. <https://doi.org/10.1016/j.fgb.2012.11.011>.
102. Vela-Corcía D, Aditya Srivastava D, Dafa-Berger A, Rotem N, Barda O, Levy M. 2019. MFS transporter from *Botrytis cinerea* provides tolerance to glucosinolate-breakdown products and is required for pathogenicity. *Nat Commun* 10:2886–2811. <https://doi.org/10.1038/s41467-019-10860-3>.
103. McDonald T, Brown D, Keller NP, Hammond TM. 2005. RNA silencing of mycotoxin production in *Aspergillus* and *Fusarium* species. *Mol Plant Microbe Interact* 18:539–545. <https://doi.org/10.1094/MPMI-18-0539>.
104. Bönnighausen J, Schauer N, Schäfer W, Bormann J. 2019. Metabolic profiling of wheat rachis node infection by *Fusarium graminearum*: decoding deoxynivalenol-dependent susceptibility. *New Phytol* 221:459–469. <https://doi.org/10.1111/nph.15377>.
105. Alexander NJ, Proctor RH, McCormick SP. 2009. Genes, gene clusters, and biosynthesis of trichothecenes and fumonisins in *Fusarium*. *Toxin Rev* 28:198–215. <https://doi.org/10.1080/15569540903092142>.
106. Kosawang C, Karlsson M, Jensen DF, Dilokpimol A, Collinge DB. 2014. Transcriptomic profiling to identify genes involved in *Fusarium* mycotoxin deoxynivalenol and zearalenone tolerance in the mycoparasitic fungus *Clonostachys rosea*. *BMC Genomics* 15:55–11. <https://doi.org/10.1186/1471-2164-15-55>.
107. Kosawang C, Karlsson M, Vélèz H, Rasmussen PH, Collinge DB, Jensen B, Jensen DF. 2014. Zearalenone detoxification by zearalenone hydrolase is important for the antagonistic ability of *Clonostachys rosea* against mycotoxigenic *Fusarium graminearum*. *Fungal Biol* 118:364–373. <https://doi.org/10.1016/j.funbio.2014.01.005>.
108. Jin JM, Lee J, Lee YW. 2010. Characterization of carotenoid biosynthetic genes in the ascomycete *Gibberella zeae*. *FEMS Microbiol Lett* 302:197–202. <https://doi.org/10.1111/j.1574-6968.2009.01854.x>.
109. Sørensen JL, Hansen FT, Sondergaard TE, Staerk D, Lee TV, Wimmer R, Klitgaard LG, Purup S, Giese H, Frandsen RJN. 2012. Production of novel fusarielins by ectopic activation of the polyketide synthase 9 cluster in *Fusarium graminearum*. *Environ Microbiol* 14:1159–1170. <https://doi.org/10.1111/j.1462-2920.2011.02696.x>.
110. Letunic I, Doerks T, Bork P. 2009. SMART 6: recent updates and new developments. *Nucleic Acids Res* 37:D229–D232. <https://doi.org/10.1093/nar/gkn808>.
111. Jones P, Binns D, Chang HY, Fraser M, Li W, McAnulla C, McWilliam H, Maslen J, Mitchell A, Nuka G, Pesseat S, Quinn AF, Sangrador-Vegas A, Scheremetjew M, Yong SY, Lopez R, Hunter S. 2014. InterProScan 5: genome-scale protein function classification. *Bioinformatics* 30:1236–1240. <https://doi.org/10.1093/bioinformatics/btu031>.
112. Marchler-Bauer A, Lu S, Anderson JB, Chitsaz F, Derbyshire MK, DeWeese-Scott C, Fong JH, Geer LY, Geer RC, Gonzales NR, Gwadz M, Hurwitz DJ, Jackson JD, Ke Z, Lanczycki CJ, Lu F, Marchler GH, Mullokandov M, Omelchenko MV, Robertson CL, Song JS, Thanki N, Yamashita RA, Zhang D, Zhang N, Zheng C, Bryant SH. 2011. CDD: a Conserved Domain Database for the functional annotation of proteins. *Nucleic Acids Res* 39:D225–D229. <https://doi.org/10.1093/nar/gkq1189>.
113. Bateman A, Martin MJ, O'Donovan C, Magrane M, Apweiler R, Alpi E, Antunes R, Arganiska J, Bely B, Bingley M, Bonilla C, Britto R, Bursteinas B, Chavali G, Cibrán-Uhalte E, Da Silva A, De Giomi M, Dogan T, Fazzini F, Gane P, Castro LG, Garmiri P, Hatton-Ellis E, Hietia R, Huntley R, Legge D, Liu W, Luo J, Maccougall A, Mutowo P, Nightingale A, Orchard S, Pichler K, Poggioli D, Pundir S, Pura L, Qi G, Rosanoff S, Saidi R, Sawford T, Shypitsyna A, Turner E, Volynkin V, Wardell T, Watkins X, Zellner H, Cowley A, Figueira L, Li W, McWilliam H, et al. 2015. UniProt: a

- hub for protein information. *Nucleic Acids Res* 43(Database Issue): D204–D212.
114. Benson DA, Cavanaugh M, Clark K, Karsch-Mizrachi I, Ostell J, Pruitt KD, Sayers EW. 2018. GenBank. *Nucleic Acids Res* 46:D41–D47. <https://doi.org/10.1093/nar/gkx1094>.
 115. Katoh K, Standley DM. 2013. MAFFT multiple sequence alignment software version 7: improvements in performance and usability. *Mol Biol Evol* 30:772–780. <https://doi.org/10.1093/molbev/mst010>.
 116. Nguyen LT, Schmidt HA, Von Haeseler A, Minh BQ. 2015. IQ-TREE: a fast and effective stochastic algorithm for estimating maximum-likelihood phylogenies. *Mol Biol Evol* 42:268–274.
 117. Rambaut A. 2018. FigTree v. 1.4.4. <http://tree.bio.ed.ac.uk/software/figtree/>.
 118. Dubey MK, Ubhayasekera W, Sandgren M, Funck Jensen D, Karlsson M. 2012. Disruption of the Eng18b ENGase gene in the fungal biocontrol agent *Trichoderma atroviride* affects growth, conidiation and antagonistic ability. *PLoS One* 7:e36152. <https://doi.org/10.1371/journal.pone.0036152>.
 119. Güldener U, Heck S, Fielder T, Beinhauer J, Hegemann JH. 1996. A new efficient gene disruption cassette for repeated use in budding yeast. *Nucleic Acids Res* 24:2519–2524. <https://doi.org/10.1093/nar/24.13.2519>.
 120. Karimi M, De Meyer B, Hilson P. 2005. Modular cloning in plant cells. *Trends Plant Sci* 10:103–105. <https://doi.org/10.1016/j.tplants.2005.01.008>.
 121. Utermark J, Karlovsky P. 2008. Genetic transformation of filamentous fungi by *Agrobacterium tumefaciens*. *Protoc Exch* 119:631–640.
 122. Dubey MK, Broberg A, Sooriyaarachchi S, Ubhayasekera W, Jensen DF, Karlsson M. 2013. The glyoxylate cycle is involved in pleiotropic phenotypes, antagonism, and induction of plant defence responses in the fungal biocontrol agent *Trichoderma atroviride*. *Fungal Genet Biol* 58–59: 33–41. <https://doi.org/10.1016/j.fgb.2013.06.008>.
 123. Knudsen IMB, Hockenhull J, Jensen DF. 1995. Biocontrol of seedling diseases of barley and wheat caused by *Fusarium culmorum* and *Bipolaris sorokiniana*: effects of selected fungal antagonists on growth and yield components. *Plant Pathol* 44:467–477. <https://doi.org/10.1111/j.1365-3059.1995.tb01669.x>.
 124. Smith CA, Want EJ, O'Maille G, Abagyan R, Siuzdak G. 2006. XCMS: processing mass spectrometry data for metabolite profiling using nonlinear peak alignment, matching, and identification. *Anal Chem* 78:779–787. <https://doi.org/10.1021/ac051437y>.
 125. Tautenhahn R, Böttcher C, Neumann S. 2008. Highly sensitive feature detection for high resolution LC/MS. *BMC Bioinformatics* 9:504–516. <https://doi.org/10.1186/1471-2105-9-504>.
 126. Hosseini P, Tremblay A, Matthews BF, Alkharouf NW. 2010. An efficient annotation and gene-expression derivation tool for Illumina Solexa datasets. *BMC Res Notes* 3:183–187. <https://doi.org/10.1186/1756-0500-3-183>.
 127. Conesa A, Götz S, García-Gómez JM, Terol J, Talón M, Robles M. 2005. Blast2GO: a universal tool for annotation, visualization, and analysis in functional genomics research. *Bioinformatics* 21:3674–3676. <https://doi.org/10.1093/bioinformatics/bti610>.
 128. Blin K, Shaw S, Steinke K, Villebro R, Ziemert N, Lee SY, Medema MH, Weber T. 2019. AntiSMASH 5.0: updates to the secondary metabolite genome mining pipeline. *Nucleic Acids Res* 47:81–87.
 129. Zhang H, Yohe T, Huang L, Entwistle S, Wu P, Yang Z, Busk PK, Xu Y, Yin Y. 2018. DbCAN2: a meta server for automated carbohydrate-active enzyme annotation. *Nucleic Acids Res* 46:95–101.
 130. Urban M, Cuzick A, Rutherford K, Irvine A, Pedro H, Pant R, Sadanadan V, Khamari L, Billal S, Mohanty S, Hammond-Kosack KE. 2017. PHI-base: a new interface and further additions for the multi-species pathogen-host interactions database. *Nucleic Acids Res* 45:D604–D610. <https://doi.org/10.1093/nar/gkw1089>.
 131. Bushnell B. 2019. BBTools: a suite of fast, multithreaded bioinformatics tools designed for analysis of DNA and RNA sequence data. Joint Genome Institute, Berkeley, CA.
 132. Dobin A, Davis CA, Schlesinger F, Drenkow J, Zaleski C, Jha S, Batut P, Chaisson M, Gingeras TR. 2013. STAR: ultrafast universal RNA-seq aligner. *Bioinformatics* 29:15–21. <https://doi.org/10.1093/bioinformatics/bts635>.
 133. Liao Y, Smyth GK, Shi W. 2014. FeatureCounts: an efficient general purpose program for assigning sequence reads to genomic features. *Bioinformatics* 30:923–930. <https://doi.org/10.1093/bioinformatics/btt656>.
 134. Love MI, Anders S, Huber W. 2014. Differential analysis of count data: the DESeq2 package. *Genome Biol* 15:550–1186. <https://doi.org/10.1186/s13059-014-0550-8>.
 135. Kopylova E, Noé L, Touzet H. 2012. SortMeRNA: fast and accurate filtering of ribosomal RNAs in metatranscriptomic data. *Bioinformatics* 28: 3211–3217. <https://doi.org/10.1093/bioinformatics/bts611>.
 136. Quast C, Pruesse E, Yilmaz P, Gerken J, Schweer T, Yarza P, Peplies J, Glöckner FO. 2013. The SILVA ribosomal RNA gene database project: improved data processing and web-based tools. *Nucleic Acids Res* 41: D590–D596. <https://doi.org/10.1093/nar/gks1219>.
 137. Paschoal AR, Maracaja-Coutinho V, Setubal JC, Simões ZLP, Verjovski-Almeida S, Durham AM. 2012. Non-coding transcription characterization and annotation: a guide and web resource for noncoding RNA databases. *RNA Biol* 9:274–282. <https://doi.org/10.4161/rna.19352>.
 138. Gremme G, Steinbiss S, Kurtz S. 2013. Genome tools: a comprehensive software library for efficient processing of structured genome annotations. *IEEE/ACM Trans Comput Biol Bioinform* 10:645–656. <https://doi.org/10.1109/TCBB.2013.68>.
 139. Mackowiak SD. 2011. Identification of novel and known unit 12.10 miRNAs in deep-sequencing data with miRDeep2. *Curr Protoc Bioinformatics* 36:12–10. <https://doi.org/10.1002/0471250953.bi1210s36>.
 140. Kozomara A, Birgaoanu M, Griffiths-Jones S. 2019. miRBase: from microRNA sequences to function. *Nucleic Acids Res* 47:155–162.
 141. The RNA Central Consortium. 2019. RNAcentral: a hub of information for noncoding RNA sequences. *Nucleic Acids Res* 47:D221–D229. <https://doi.org/10.1093/nar/gky1034>.
 142. Chen R, Jiang N, Jiang Q, Sun X, Wang Y, Zhang H, Hu Z. 2014. Exploring microRNA-like small RNAs in the filamentous fungus *Fusarium oxysporum*. *PLoS One* 9:e104956. <https://doi.org/10.1371/journal.pone.0104956>.
 143. Devers EA, Branscheid A, May P, Krajinski F. 2011. Stars and symbiosis: microRNA- and microRNA*-mediated transcript cleavage involved in arbuscular mycorrhizal symbiosis. *Plant Physiol* 156:1990–2010. <https://doi.org/10.1104/pp.111.172627>.
 144. Wang L, Xu X, Yang J, Chen L, Liu B, Liu T, Jin Q. 2018. Integrated microRNA and mRNA analysis in the pathogenic filamentous fungus *Trichophyton rubrum*. *BMC Genomics* 19:933–914. <https://doi.org/10.1186/s12864-018-5316-3>.
 145. Xia Z, Wang Z, Kav NNV, Ding C, Liang Y. 2020. Characterization of microRNA-like RNAs associated with sclerotial development in *Sclerotinia sclerotiorum*. *Fungal Genet Biol* 144:103471. <https://doi.org/10.1016/j.fgb.2020.103471>.
 146. Rueda A, Barturen G, Lebrón R, Gómez-Martín C, Alganza Á, Oliver JL, Hackenberg M. 2015. SRNAToolbox: an integrated collection of small RNA research tools. *Nucleic Acids Res* 43:W467–W473. <https://doi.org/10.1093/nar/gkv555>.
 147. Enright A, John B, Gaul U, Tuschl T, Sander C, Marks D. 2003. MicroRNA targets in *Drosophila*. *Genome Biol* 4:P8–P27. <https://doi.org/10.1186/gb-2003-4-11-p8>.
 148. Kertesz M, Iovino N, Unnerstall U, Gaul U, Segal E. 2007. The role of site accessibility in microRNA target recognition. *Nat Genet* 39:1278–1284. <https://doi.org/10.1038/ng2135>.
 149. Sturm M, Hackenberg M, Langenberger D, Frishman D. 2010. TargetSpy: a supervised machine learning approach for microRNA target prediction. *BMC Bioinformatics* 11:292–217. <https://doi.org/10.1186/1471-2105-11-292>.
 150. Wu H-J, Ma Y-K, Chen T, Wang M, Wang X-J. 2012. PsRobot: a web-based plant small RNA meta-analysis toolbox. *Nucleic Acids Res* 40:W22–W28. <https://doi.org/10.1093/nar/gks554>.
 151. Bonnet E, He Y, Billiau K, Van de Peer Y. 2010. TAPIR, a web server for the prediction of plant microRNA targets, including target mimics. *Bioinformatics* 26:1566–1568. <https://doi.org/10.1093/bioinformatics/btq233>.
 152. Amselem J, Cornut G, Choisne N, Alaux M, Alfama-Depauw F, Jamilloux V, Maumus F, Letellier T, Luyten I, Pommier C, Adam-Blondon AF, Quesneville H. 2019. RepetDB: a unified resource for transposable element references. *Mob DNA* 10:6. <https://doi.org/10.1186/s13100-019-0150-y>.
 153. Kodama H, Komamine A. 2011. RNAi and plant gene function analysis. Springer, New York, NY.
 154. Livak KJ, Schmittgen TD. 2001. Analysis of relative gene expression data using real-time quantitative PCR and the 2^{-ΔΔCT} method. *Methods* 25: 402–408. <https://doi.org/10.1006/meth.2001.1262>.